PERGAMON

Neural Networks 14 (2001) 955–975

Neural Networks

www.elsevier.com/locate/neunet

2001 Special issue

Is the integrate-and-fire model good enough?—a review

Jianfeng Feng*

COGS, Sussex University, Brighton, Sussex BN1 9QH, UK

Received 10 October 2000; revised 11 April 2001; accepted 11 April 2001

Abstract

We review some recent results on the behaviour of the integrate-and-fire (IF) model, the FitzHugh–Nagumo (FHN) model, a simplified version of the FHN (IF-FHN) model and the Hodgkin–Huxley (HH) model with correlated inputs. The effect of inhibitory inputs on the model behaviour is also taken into account. Here, inputs exclusively take the form of diffusion approximation and correlated inputs mean correlated synaptic inputs (Sections 2 and 3). It is found that the IF and HH models respond to correlated inputs in totally opposite ways, but the IF-FHN model shows similar behaviour to the HH model. Increasing inhibitory input to single neuronal models, such as the FHN model and the HH model can sometimes increase their firing rates, which we termed inhibition-boosted firing (IBF). Using the IF model and the IF-FHN model, we theoretically explore how and when IBF can happen. The computational complexity of the IF-FHN model is very similar to the conventional IF model, but the former captures some interesting and essential features of biophysical models and could serve as a better model for spiking neuron computation.

Keywords: The integrate-and-fire model; The Hodgkin-Huxley model; The Fitzhugh-Nagumo model; The IF-FHN model; Inhibition boosted firing

1. Introduction

The two most commonly used single neuron models in theoretical neuroscience are the integrate-and-fire model (IF), modelling neurons at an abstract level and the Hodgkin–Huxley (HH) model describing the biophysical mechanisms of cells. Recently, it has been found (Brown, Feng & Feerick, 1999; Feng, 1997; Feng & Brown, 2000b) that in certain parameter regions the coefficient of variation (CV = mean/standard deviation) of efferent spike trains of the HH model is almost independent of the ratio between inhibitory and excitatory inputs. In other words, whether inhibitory inputs are blocked or not has no effect on the CV. However, most results to date on the IF and HH models are obtained under the assumption that inputs are independent (Brown et al., 1999; Feng, 1997; Tuckwell, 1988), both spatially (synaptically) and temporally. This assumption obviously contradicts the physiological data that clearly show that nearby neurones usually fire in a correlated way (Zohary, Shadlen & Newsome, 1994), and the anatomical data that reveal that neurons with similar functions group together and fire together. In fact 'firing together, coming together' is a basic principle in neuronal development (Sheth, Sharma, Rao & Sur, 1996). Furthermore, data in Zohary et al., 1994) indicate that even a weak correlation within a population of neurons can have a dramatic impact on the network behaviour. The essential role played by redundancy or correlation in perception was appreciated early in the literature (Barlow, 1986). Hence, it is of crucial importance to explore the impact of weakly correlated synaptic inputs on the efferent spike trains of neuronal models, which certainly sheds new light on the coding problem (Albright, Jessell, Kandel & Posner, 2000; Shadlen & Movshon, 1999).

For the IF model, the output firing variability, measured by CV, is an increasing function of input correlation: the larger the input correlation, the larger the CV of efferent spike trains. It is surprising to find that the correlation in input signals has a totally *opposite* effect on the CV of efferent spike trains of the HH model: the correlation in inputs reduces rather than increases the CV of efferent spike trains. Furthermore, with fixed correlation, the CV of efferent spike trains is almost independent of the ratio between inhibitory and excitatory inputs. Hence, the IF and HH models operate in two quite different modes: increasing the input correlation will decrease the signal to noise ratio of efferent spike trains in the IF model; whereas for the HH model an enhancement on the signal to noise ratio is attained. We thus conclude that the IF model works better in an environment of asynchronous inputs, but the HH model has an advantage for more synchronous (correlated) inputs. All the conclusions for the HH model are then repeated for the FHN model. The IF-FHN model (Feng &

* Tel.: +44-1273-606755; fax: +44-1273-671320.
E-mail address: jf218@cam.ac.uk (J. Feng).

0893-6080/01/$ - see front matter
PII: S0893-6080(01)00074-0

Brown, 2000a) is employed to show that the differences between the IF model and the HH model result from the fact that the former model has a constant decay rate, but the latter has a non-constant decay rate.

Why neurons in the cortex receive and emit stochastic rather than deterministic signals remains elusive, despite century-long research activity. The stochastic part of a signal is usually thought of as 'noise' and is the part any system tries to get rid of. In stochastic resonance theory (Collins, Chow & Imhoff, 1995; Gammaitoni, Hänggi, Jung & Marchesoni, 1998), noise is hypothesized to be useful, but an application of the theory to the neuronal system tells us that it only works inside a very limited parameter region and a carefully adjusted input signal is required (Feng & Tirozzi, 2000). Another possible role played by noise in neuronal systems has been reported recently: we (Feng & Zhang, 2001) have *numerically* demonstrated that with the help of noise, a neuron, such as the HH and the FHN model, can *increase* its efferent firing rate when inhibitory inputs *increase*. As in the literature (Brown et al., 1999; Feng, 1997; Feng & Zhang, 2001), we assume that a neuron receives inputs ranging from purely excitatory inputs to exactly balanced inhibitory and excitatory inputs.

A natural and interesting question is then, why and when increasing inhibitory inputs to a neuron can boost its efferent firing rate. Surprisingly, the IBF (inhibition-boosted firing) phenomenon is observable for both the IF and IF-FHN models, which indicates that the IBF is not due to complex, nonlinear mechanisms of biophysical models. We apply theoretical results recently developed in Feng and Li (2000) to the IF model and the IF-FHN model. The approach enables us to prove that when input frequency is lower than a critical frequency, the output frequency is higher when the neuron receives a mixture of inhibitory and excitatory inputs than when it receives purely excitatory inputs. Moreover, the critical frequency is unique. For the IF-FHN model we apply Kramer's formula to prove that there is a critical frequency at which the efferent firing rate, when the model receives purely excitatory inputs, is equal to the rate with exactly balanced inputs.

We then propose a simple approach called response surface to *graphically* explore the different behaviour between the IF, IF-FHN and HH models with correlated inputs and the IBF phenomenon. The response surface method enables us to grasp the property of a neuron with stochastic inputs and unify the aforementioned results. The response surface of a simple version of the response spike model (Kistler, Gerstner & van Hemmen, 1997) is also included. We advocate that the approach could also be applied in experiments.

The paper is organized as follows. In Section 2, the IF model and the HH model are introduced. In Section 3, correlated synaptic inputs are defined. Section 4 is devoted to numerical results of the IF model, the HH model and the FHN model with correlated inputs. In Section 5, the IF-FHN model is briefly reviewed (Feng & Brown, 2000a), its behaviour with correlated inputs is shown and a comparison with other models such as Abbott–Kepler's model (Abbott & Kepler, 1990) and the spike response model (Kistler et al., 1997) is included. In the present paper, we exclusively restrict ourselves to the models with diffusion approximations to Poisson, positively correlated inputs and refer the reader to Feng and Tirozzi (2000) for the negatively correlated input case. Commencing from Section 6 we turn our attentions to the IBF phenomenon. Section 6 is devoted to numerical examples. In Section 7, theoretical results on both the IF and IF-FHN models are included. Section 8 is devoted to finding out exactly the IBF regions of parameters. Section 9 considers the IBF phenomenon with correlated inputs. The response surface approach is introduced in Section 10 and applied to the IF model, the HH model, the IF-FHN model and a simplified version of the spike response model.

2. The integrate-and-fire model and the Hodgkin–Huxley model

Suppose that a cell receives EPSPs (excitatory postsynaptic potentials) at p synapses and IPSPs (inhibitory postsynaptic potentials) at q inhibitory synapses. The activities among excitatory synapses and inhibitory synapses are correlated but, for simplicity of notation only, are assumed to be independent between them. When the membrane potential V_t is between the resting potential V_{rest} and the threshold V_{thre}, it is given by

$$\mathrm{d}V_t = -L(V_t - V_{\text{rest}})\mathrm{d}t + \mathrm{d}\bar{I}_{\text{syn}}(t) \tag{2.1}$$

where L is the decay rate and synaptic inputs

$$\bar{I}_{\text{syn}}(t) = a\sum_{i=1}^{p} E_i(t) - b\sum_{j=1}^{q} I_j(t)$$

with $E_i(t), I_i(t)$ as a Poisson processes with rate λ_{E} and λ_{I}, respectively, $a > 0$, $b > 0$ being the magnitude of each EPSP and IPSP. Once V_t crosses V_{thre} from below, a spike is generated and V_t is reset to V_{rest}. This model is termed the IF model. The inter-spike interval of efferent spikes is

$$T = \inf\{t : V_t \geq V_{\text{thre}}\}$$

For simplicity of notation, we assume that the correlation coefficient between the i-th excitatory (inhibitory) synapse and the j-th excitatory (inhibitory) synapse is $c(i,j) = \rho(\|i-j\|)$, where ρ is a non-increasing function. The correlation considered here reflects the correlation of activity of different synapses, as discussed and explored in Feng and Brown, 2000b; Salinas and Sejnowski, 2000; Stevens and Zador, 1998a. It is not the correlation of single incoming EPSP or IPSP that could be expressed as $c_{ij}(t-t')$ for the EPSP (IPSP) at time t of the i-th synapse and time t' of the j-th synapse. We refer the reader to Feng and Brown (2000b) for a detailed discussion on the meaning of the correlation considered here.

A slightly more general model than the IF model defined above is the IF model with reversal potentials

defined by

$$dZ_t = -(Z_t - V_{rest})Ldt + d\bar{I}_{syn}(Z_t, t) \quad (2.2)$$

where

$$\bar{I}_{syn}(Z_t, t) = \bar{a}(V_E - Z_t)\sum_{i=1}^{p} E_i(t) + \bar{b}(V_I - Z_t)\sum_{j=1}^{q} I_j(t)$$

V_E and V_I are the reversal potentials $V_I < V_{rest} < V_E$, $\bar{a}(V_E - V_{rest})$, $\bar{b}(V_I - V_{rest})$ are the magnitude of single EPSP and IPSP when $Z_t = V_{rest}$. Z_t (membrane potential) is now a birth-and-death process with boundaries V_E and V_I.

We consider the classic HH model with correlated inputs given by

$$CdV = -g_{Na}m^3h(V - V_{Na})dt - g_K n^4(V - V_K)dt - g_L(V - V_L)dt + dI_{syn}(V, t) \quad (2.3)$$

where $I_{syn}(V, t) = \bar{I}_{syn}$ or $I_{syn}(V, t) = \bar{I}_{syn}(V, t)$. Equations and parameters used in the HH model are as follows (Abbott, 1994; Brown et al., 1999).

$$\frac{dn}{dt} = \frac{n_\infty - n}{\tau_n}, \qquad \frac{dm}{dt} = \frac{m_\infty - m}{\tau_m}, \qquad \frac{dh}{dt} = \frac{h_\infty - h}{\tau_h}$$

and

$$n_\infty = \frac{\alpha_n}{\alpha_n + \beta_n}, \qquad m_\infty = \frac{\alpha_m}{\alpha_m + \beta_m},$$

$$h_\infty = \frac{\alpha_h}{\alpha_h + \beta_h}\tau_n, \qquad = \frac{1}{\alpha_n + \beta_n}, \qquad \tau_m = \frac{1}{\alpha_m + \beta_m},$$

$$\tau_h = \frac{1}{\alpha_h + \beta_h}$$

with

$$\alpha_n = \frac{0.01(V + 55)}{1 - \exp\left(-\frac{V + 55}{10}\right)},$$

$$\beta_n = 0.125\exp\left(-\frac{V + 65}{80}\right),$$

$$\alpha_m = \frac{0.1(V + 40)}{1 - \exp\left(-\frac{V + 40}{10}\right)}, \qquad \beta_m = 4\exp\left(-\frac{V + 65}{18}\right),$$

$$\alpha_h = 0.07\exp\left(-\frac{V + 65}{20}\right), \qquad \beta_h = \frac{1}{\exp\left(-\frac{V + 35}{10}\right) + 1}$$

The parameters used in Eq. (2.3) are $C = 1$. $g_{Na} = 120$, $g_K = 36$, $g_L = 0.3$, $V_K = -77$, $V_{Na} = 50$, $V_L = -54.4$.

3. Synaptic inputs

Here, we use the usual diffusion approximation to approximate the IF models with or without reversal potentials, or more exactly the synaptic inputs of the models (see below). We do not check the approximation accuracy because it has been done by many authors (Ricciardi & Sato, 1990; Tuckwell, 1988).

The input now reads

$$E_i(t) \sim \lambda_E t + \sqrt{\lambda_E}B_i^E(t)$$

and similarly

$$I_i(t) \sim \lambda_I t + \sqrt{\lambda_I}B_i^I(t)$$

where $B_i^E(t)$ and $B_i^I(t)$ are standard Brownian motions. The approximation above is called the diffusion approximation because the right-hand-sides the of equations are diffusion processes (continuous processes). We note that the diffusion process $\lambda_E t + \sqrt{\lambda_E}B_i^E(t)$ and the jump process $E_i(t)$ share identical first and second order statistics. Therefore, the IF model without reverse potentials can be approximated by

$$dv_t = -L(v_t - V_{rest})dt + d\bar{i}_{syn}(t)$$

where

$$\bar{i}_{syn}(t) = a\sum_{i=1}^{p}\lambda_E t - b\sum_{j=1}^{q}\lambda_I t + a\sqrt{\lambda_E}\sum_{i=1}^{p}B_i^E(t) - b\sqrt{\lambda_I}\sum_{j=1}^{q}B_j^I(t) \quad (3.1)$$

Since the summation of Brownian motions is again a Brownian motion we can rewrite the equation above as follows

$$\bar{i}_{syn}(t) = \mu(t) + \sigma B(t) \quad (3.2)$$

where $B(t)$ is a standard Brownian motion

$$\mu = ap\lambda_E - bq\lambda_I,$$

$$\sigma^2 = a^2p\lambda_E + b^2q\lambda_I + a^2\lambda_E\sum_{i\neq j}^{p}c(i,j) + b^2\lambda_I\sum_{i\neq j}^{q}c(i,j) \quad (3.3)$$

Now, we turn our attention to the IF model with reversal potentials. Similar to what we have done for the IF model without reversal potentials, we can rewrite the model in the following form

$$dz_t = -Lz_t dt + d\bar{i}_{syn}(z_t, t) \quad (3.4)$$

where

$$\bar{i}_{syn}(z_t, t) = (ap(V_E - z(t))\lambda_E - bq(z(t) - V_I)\lambda_I)t + \sigma(z_t)B(t)$$

and

$$\sigma^2(z_t) = a^2(z_t - V_E)^2p\lambda_E + b^2(z_t - V_I)^2q\lambda_I + a^2(z_t - V_E)^2\lambda_E\sum_{i\neq j}^{p}c(i,j) + b^2(z_t - V_I)^2\lambda_I\sum_{i\neq j}^{q}c(i,j)$$

There are other forms of the diffusion terms in Eq. (3.4) to approximate the original process (Musila & Lánsky, 1994). For simplicity of notation, we confine ourselves to $\sigma^2(z_t)$.

For the HH model, we have analogous expressions for correlated inputs with or without reversal potentials as in Eq. (3.2), i.e. $\bar{I}_{\text{syn}}(t)$ and Eq. (3.4), i.e. $\bar{I}_{\text{syn}}(v,t)$.

In the sequel, we confine ourselves to the case of inputs without reversal potentials. Nevertheless all results are qualitatively true for the models with inputs with reversal potentials.

4. Numerical results

From the results above, we conclude that correlated inputs increase the variance of inputs and, thus, we expect an increase of CV of efferent inter-spike intervals is attained for the IF model (Feng & Brown, 2000b; Shadlen & Newsome, 1998). For the HH model, an analytical treatment is difficult and we have to resort to numerical simulations. Here, only results of the case that $c(i,j)=c$ for $i\neq j$, $i, j=1,\ldots,p$ and $c(i,j)=c$ for $i\neq j$, $i,j=1,\ldots,q$ for the models without reverse potentials are presented. It has been reported in the literature that the correlation coefficient between cells is around 0.1 in V5 of rhesus monkeys in vivo (Zohary et al., 1994), and around 0.2 in human motor units of a variety of muscles (Matthews, 1996).

Fig. 1 shows numerical results of the IF model and the HH model with c between 0 and 0.1, and $q=0, 10, \ldots, 100$. We first look at the results for the IF model (Fig. 1A). When $c=0$, inputs without correlation, there are many numerical and theoretical investigations (see for example,Brown et al., 1999; Feng, 1997; Feng & Brown, 2000a,b; Softky & Koch, 1993). In line with the theoretical results above, the larger the input correlation is, the larger is the output CV. In particular, we note that when $c>0.08$ we have CV >0.5 for any value of q. In conclusion, with a fixed p, CV is an increasing function of the correlation and the number of inhibitory inputs. However, for the HH model, the situation is totally different (Fig. 1B): for fixed correlation coefficients, CV is almost a constant, independent of the number of inhibitory inputs; for fixed number of inhibitory inputs, CV is a *decreasing* function of the input correlation. In other words, for the HH model, the stronger the input correlation is (equivalent to a stronger input noise), the more regular is the output.

In recent years, there has been much research devoted to the problem of how to generate efferent spikes with a CV between 0.5 and 1 (see for example Brown et al., 1999; Feng, 1997; Feng & Brown, 2000a,b; Feng & Tirozzi, 2000; Konig, Engel & Singer, 1996; Shadlen & Newsome, 1994; Softky & Koch, 1993). In particular, it is pointed out in Softky and Koch (1993) that it is impossible for the IF model and some biophysical models to generate spikes with a CV between 0.5 and 1 if the inputs are exclusively excitatory and independent. This phenomenon is referred to as

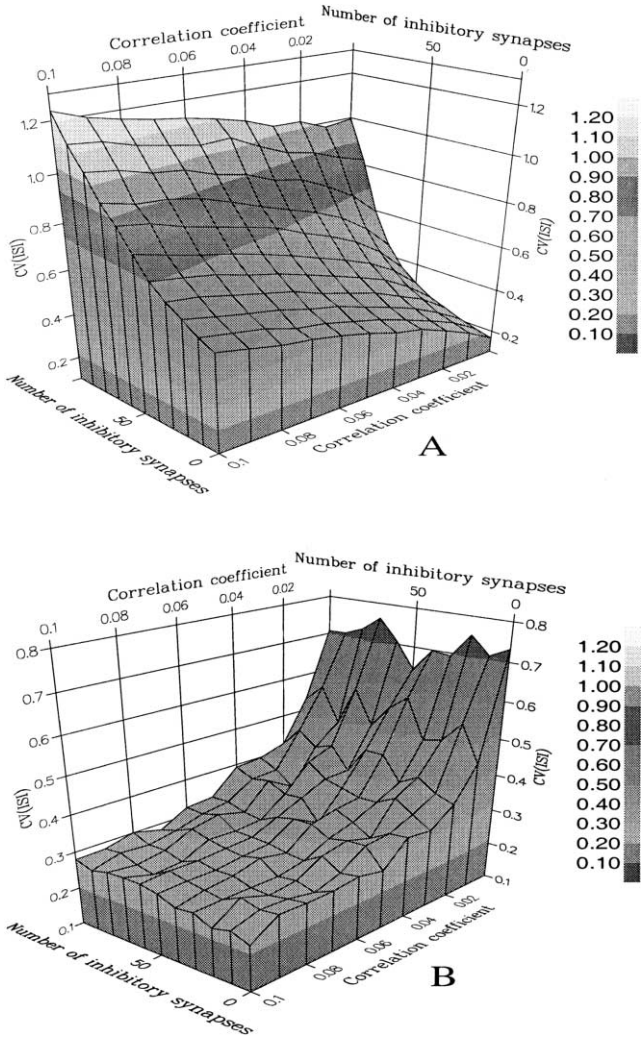

Fig. 1. CV versus correlation and q. Data are obtained by simulating the IF model (A) and the HH model (B) with synaptic input $\bar{I}(t)$. $A=b=0.5$ mV, $\lambda_I=\lambda_E=100$ Hz, $V_{\text{rest}}=0$ mV, $V_{\text{thre}}=20$ mV, $1/L=20.2$ ms, $p=100$, $q=0, 10, \ldots, 100$. For the reason behind the choice of these parameters we refer the reader to Brown et al. (1999), Feng (1997) and Feng and Brown (2000b).

the 'central limit effect' and widely cited in the literature (see for example Abbott, Varela, Sen & Nelson, 1997). Many different approaches have been proposed to get around this problem. In the present paper, we clearly demonstrate that even with exclusively excitatory inputs the IF model is capable of emitting spike trains with a CV greater than 0.5. Under the condition that $c>0.08$ (Fig. 1A), no matter what the ratio is between the excitatory and inhibitory synapses, the CV of efferent spike trains is always greater than 0.5. For the HH model when the input correlation is low, independent of the inhibitory inputs, the output CV is always greater than 0.5.

There is increasing evidence to support the assumption that the brain might use different coding strategies when dealing with tasks of different complexity. When a slow reaction is required, the brain might use rate coding to

process information. When a fast reaction is needed, the brain only has enough time to take into account the first spike of active synapses and so temporal coding seems more plausible. This assumption naturally requires that neurons operate in different modes. Under the rate coding assumption, here we provide an example of different operation modes, provided that both the IF and the HH mechanisms are employed by cells in the brain. The IF model is sensitive to its input correlation and so it would work in an environment of less correlated or asynchronous inputs. The HH model is more reliable when correlated or synchronized inputs are presented. Fig. 2 (see Fig. 15) shows a case of signal to noise ratio of efferent spike trains, i.e. mean/standard deviation or 1/CV. When input correlation is small the SNR = 1/CV of the IF model is greater than that of the HH model, but when it is larger, the SNR of the IF model is less than that of the HH model.

Note that the above properties of SNR are true for all parameter regions we considered (see next section), whether or not its CV is greater than 0.5. Hence, when we restrict ourselves to the parameter regions of irregular firing: for the HH model with a fixed number of inhibitory inputs, the SNR is an *increasing* function of the input correlation; for the IF model with a fixed number of inhibitory inputs, the SNR is a *decreasing* function of the input correlation. All considerations here are based upon our simulations of the model with stationary inputs of fixed EPSP rates. The conclusion remains true for a non-stationary input if the input is not far away from the stationary input region we considered. When the input firing rate is very small where the IBF could occur, the conclusion may change (see Section 10).

An obvious difference between the integrate-and-fire model and the HH model lies in the fact that the latter has a refractory period of about 12.2 ms (Brown et al., 1999). We also add refractory periods to the integrate-and-fire model for calculating related quantities and all the results above remain true (see next section). In fact, from Fig. 2 we conclude that adding a refractory period to the IF model will even increase the discrepancy between the two models. According to the definition of SNR, we know that $\overline{SNR} = SNR + R/SD$, where $\overline{SNR}$ is obtained after adding a refractory period R, and SD is the standard deviation of inter-spike intervals of the IF model. Since SD is an increasing function of correlations, we see that $\overline{SNR}$ will decrease more sharply than the SNR of the IF model shown in Fig. 2, resulting in even larger differences between the two models. Different refractory periods for the HH model have been reported, depending on inputs (for example, it is about 15 ms in Kistler et al., 1997). It is readily seen that our conclusions above are independent of the exact value of the refractory period.

Essentially, it is impossible to have an analytical treatment of the HH model. For confirmation of our results on the HH model, we also simulated the HH model in NEURON (Hines & Carnevale, 1995) with synaptic inputs as a square wave of magnitude of 5 μA, duration 0.1 ms (Brown et al., 1999). The results match approximately with Fig. 1B. For both models, we have carried out systematic simulations on a wide range of parameters: $p = 75$, 100, 150, 200 and $0 \le r = q/p \le 1$. The results obtained qualitatively agree with the conclusions above.

We also simulate another simplified model, the Fitz-Hugh–Nagumo model which mimics the HH model, with correlated inputs. Fig. 3 shows that all the above conclusions for the HH model are true for the Fitz-Hugh–Nagumo model. The FitzHugh–Nagumo model

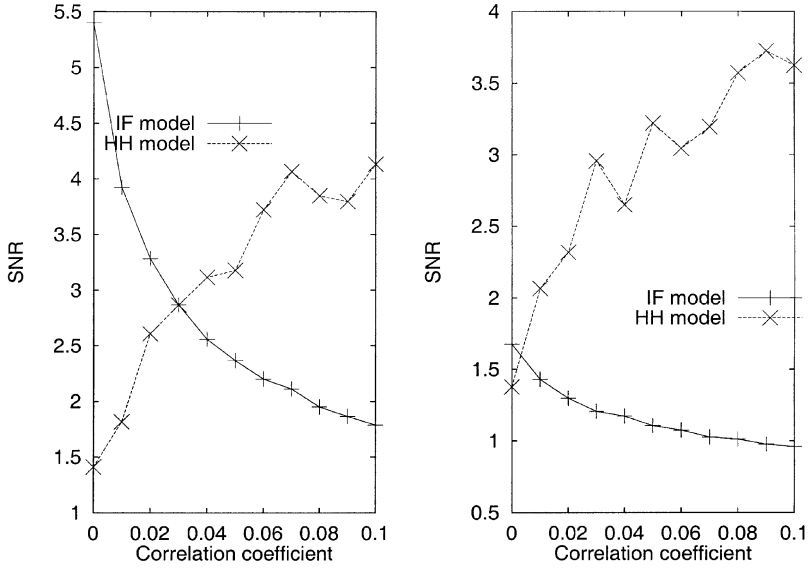

Fig. 2. Signal to noise ratio (SNR) of efferent spike trains of the IF model and the HH model comparing Fig. 1. Left figure corresponds to the case of 1/CV with fixing $q = 10$ in Fig. 1; right figure with fixing $q = 80$.

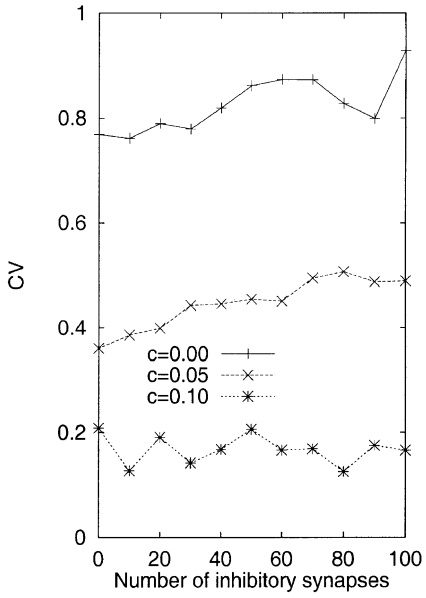

Fig. 3. CV versus q for the FitzHugh–Nagumo model with correlated inputs, $p = 100$, $\lambda_E = \lambda_I = 100$ Hz.

is described by

$$\begin{aligned} dv &= \gamma[-v(v-\alpha)(v-1) - w]dt + d\bar{i}_{syn}, \\ dw &= \delta[v - \beta w]dt \end{aligned} \tag{4.1}$$

with $\alpha = 0.2$, $\beta = 2.5$, $\gamma = 100$, $\delta = 0.25$, $a = b = 0.06$ in $\bar{i}_{syn}$ and all other parameters are the same as in the HH model.

All numerical simulations for the IF model are carried out with synaptic inputs defined by Eq. (3.2) with a time step 0.01 and a Euler scheme. For the HH model, an algorithm for solving stiff equations from the NAG library is used with step size 0.01. Further small time steps are used and we conclude no significant improvements are obtained. When calculating the mean firing rate and CV, 10,000 inter-spike intervals are employed.

5. IF-FHN model

5.1. The model

In order to theoretically understand the results presented in the previous sections, we consider the IF-FHN model, which mimics the FHN model and is proposed in Feng and Brown (2000a), with correlated inputs. Firstly, we briefly review the model.

The basic idea to derive the IF-FHN model is that to develop a systematic approach to approximating biophysical models by models of the integrate-and-fire type. The two essential components of the leaky integrate-and-fire model are *integration of incoming signals* and *leakage*. Our approach is then to determine terms which reflect these two components for a given biophysical model as exactly as possible. Devising methods for approximating biophysical models by abstract models—which preserve the essential complexity of the biophysical mechanism, yet are simultaneously concise and transparent—is an important continuing task in computational neuroscience. The advantages are obvious. Biophysical models are usually difficult to understand, and to simulate at a network level, characteristics not shared, for example, by the conventional integrate-and-fire (IF) model. A simplified expression might also provide us with a new tool to understand the frequently puzzling behaviour of biophysical models, since the response of the conventional leaky integrate-and-fire type model to stochastic input is more comprehensible. Although a rigorous analytical treatment is difficult, various approximations are available (see for example, Ricciardi & Sato, 1990).

As an application of the idea above, we consider the FitzHugh–Nagumo (FHN) model. We first define leakage coefficient as precisely as possible in this more general context. Consider a general model,

$$dv(t) = f(v,w)dt, \qquad dw(t) = g(v,w)dt \tag{5.1}$$

in which v is membrane potential, w is a vector recovery variable, generally representing activation and inactivation variables for the ion channels in the model. Luckily, in neural models, for example the Morris–Lecar or the HH model, the function g (channel activities, i.e. the master equation of a Markov process) is usually linear and so we can solve it analytically. Substituting the solution of it, or them, into the equation of f, which is different for different models and is usually highly nonlinear, and using Taylor expansion, we can obtain an integrate-and-fire model with nonlinear leakage. Therefore, our aim in achieving an integrate-and-fire reduction is to re-express the model as follows

$$dv(t) = -L(v)(v - v_{rest})dt \tag{5.2}$$

where v_{rest} is the resting potential, $L(v)$ is the *generalized leakage coefficient*. In the extreme case, for the conventional leaky integrate-and-fire model, the model is extremely simple

$$dv(t) = -L(v - v_{rest})dt \tag{5.3}$$

where the leakage coefficient L is a constant, independent of the values of v. In general, it will only be possible to express a model in the form of Eq. (5.2) approximately.

Now, we mimic the FHN model with leaky integrate-and-fire type model. First of all, we see that the second differential equation of the FHN model can be solved as follows

$$w(t) = \delta \int_0^t v(s)\exp(-\beta\delta(t-s))ds \tag{5.4}$$

Substituting Eq. (5.4) into the first differential equation

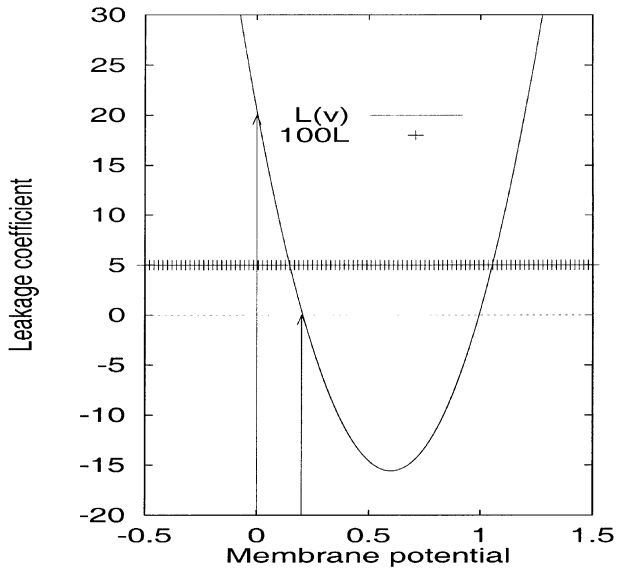

Fig. 4. $L(v)$ and $100L = 5$ versus the membrane potentials. Between the threshold and the resting potential (indicated by arrows), $L(v)$ are positive, but the closer the membrane potential to the threshold, the weaker the leakage, in contrast to the conventional integrate-and-fire model.

of the FHN model we obtain[1]

$$\mathrm{d}v(t) = -\gamma(v-1)(v-\alpha)v\mathrm{d}t - \delta\int_0^t v(s)\exp(-\beta\delta(t-s))\mathrm{d}s + \mathrm{d}\bar{i}_{\mathrm{syn}}(t) \tag{5.5}$$

Using our basic idea—to extract the leakage coefficient from the FHN model as exactly as possible, i.e. to rewrite this differential equation in the form

$$\mathrm{d}v(t) = -L(v)(v - v_{\mathrm{rest}})\mathrm{d}t \tag{5.6}$$

we rewrite Eq. (5.5) as follows

$$\begin{aligned}\mathrm{d}v(t) &= -\left[\gamma(v-1)(v-\alpha) + \delta\int_0^t \exp(-\beta\delta(t-s))\mathrm{d}s\right]v(t)\mathrm{d}t \\ &\quad - \delta\int_0^t (v(s)-v(t))\exp(-\beta\delta(t-s))\mathrm{d}s\mathrm{d}t + \mathrm{d}\bar{i}_{\mathrm{syn}}(t) \\ &= -\left[\gamma(v-1)(v-\alpha) + \frac{1}{\beta}(1-\exp(-\beta\delta t))\right]v(t)\mathrm{d}t \\ &\quad - \delta\int_0^t (v(s)-v(t))\exp(-\beta\delta(t-s))\mathrm{d}s\mathrm{d}t + \mathrm{d}\bar{i}_{\mathrm{syn}}(t)\end{aligned} \tag{5.7}$$

Note that in Eq. (5.7) the term

$$\delta\int_0^t (v(s)-v(t))\exp(-\beta\delta(t-s))\mathrm{d}s$$

is a higher order term, that we could omit in the first order approximation. Eq. (5.7) becomes

$$\mathrm{d}v(t) = -\left[\gamma(v-1)(v-\alpha) + \frac{1}{\beta}(1-\exp(-\beta\delta t))\right]v(t)\mathrm{d}t + \mathrm{d}\bar{i}_{\mathrm{syn}}(t) \tag{5.8}$$

Let us define

$$L(v) = \gamma(v-1)(v-\alpha) + \frac{1}{\beta} \tag{5.9}$$

which gives us the leakage coefficient (approximated to the first order) extracting from the FHN model.

Fig. 4 depicts a typical case of the leakage coefficient extracted from the FHN model. When the membrane potential is between the resting potential V_{rest}~0 and the threshold V_{thre}~α (indicated by arrows), the leakage coefficient is positive. Hence, the system will gradually lose its memory of recent activation. However, $L(v)$ is very different from L, which is a constant and is independent of its membrane potentials. $L(v)$ is larger when the membrane potential is close to the resting potential, and vanishes when the membrane potential is close to the threshold. In other words, when the membrane potential is near resting potential, the model loses its memory rapidly. Incoming signals accumulate less effectively to increase membrane potential. When the membrane potential is near the threshold, however, the FHN model behaves more like a perfect integrate-and-fire model. The FHN now has a very good 'memory' and in a sense 'waits' just below the threshold. As soon as some positive signals arrive, the neuron fires. Therefore, below the threshold, the IF-FHN behaves as a combination of the *leaky* integrate-and-fire model and the *perfect* integrate-and-fire model.

Once the membrane potential is above the threshold, $L(v)$ acts as an amplifier of the incoming signal, rather than as a leakage. It will increase membrane potential until it arrives at its maximum value, designated as v_{h} in this paper, and then $L(v)$ becomes positive again.

Now, we are in the position to define the following dynamics as the integrate-and-fire model with nonlinear leakage (IF-FHN) (Feng & Brown, 2000a):

$$\mathrm{d}v_t = -L(v)v\mathrm{d}t + \mathrm{d}\bar{i}_{\mathrm{syn}}(t), \qquad v_0 = V_{\mathrm{rest}} \tag{5.10}$$

For a prefixed *threshold* v_{h}, once v crosses it from below, v is then reset to v_{rest}. Unlike the conventional integrate-and-fire model, the IF-FHN increases to v_{h} rather than V_{thre}, which is smaller than v_{h}.

We use the set of parameters as before. What is the behaviour of the IF-FHN? In Fig. 5 we see that CV(ISI) is quite high and is not sensitive to the number of inhibitory inputs, similar to what we have observed for the FHN model itself (Brown et al., 1999). However, in Brown et al. (1999) we were not able to elucidate the mechanism which ensures the occurrence of the phenomenon. Based upon the numerical results on the IF-FHN model, we conclude that the nonlinear

[1] Note that to keep the derived model operating in the similar region of the FHN model, we have set γ in front of w being 1.

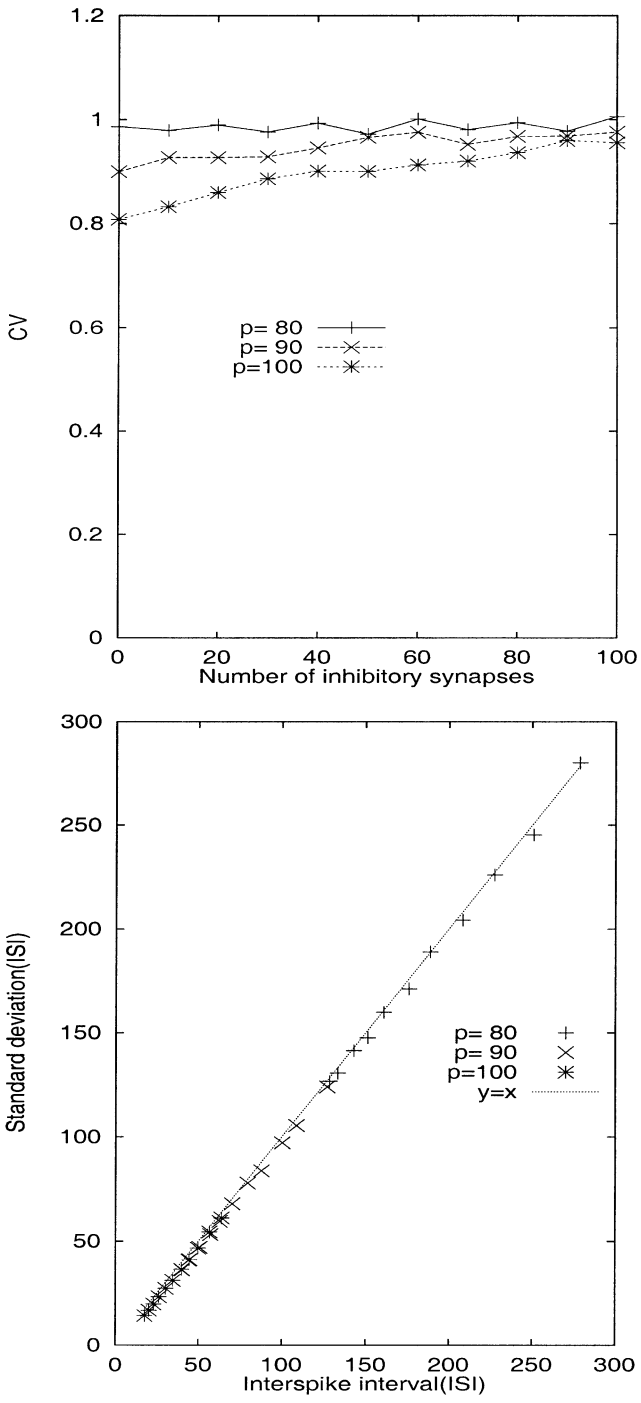

Fig. 5. CV versus q and standard deviation of inter-spike intervals versus mean inter-spike intervals of the IF-FHN model. With respect to varying q, CV (calculated after adding a refractory period of 3.2 ms) is quite flat. Note that the standard deviation almost equals the mean inter-spike interval.

leakage coefficient contributes to the flat CV, which is a typical feature of some biophysical models and which is not captured by conventional integrate-and-fire models.

To further demonstrate the power of our approach, we consider the models with correlated inputs. The IF model is essentially a linear model and so the larger is its input fluctuation, the larger is its output variety, but biophysical models such as the FHN and Hodgkin–Huxley models exhibit the opposite behaviour. This phenomenon is of particular interest. Biophysical models such as the FHN and the Hodgkin–Huxley models improve their performance in an environment of correlated inputs, which is certainly an extremely possible case in a neuronal assembly. The phenomenon is also the main motivation of our present approach in this section per se: to find integrate-and-fire type models which are qualitatively in agreement with biophysical models. Suppose that the correlation between synapses is $c > 0$. Fig. 6 clearly shows how the contradiction between biophysical models and the integrate-and-fire type model is resolved. Our simulations further confirm that the key difference between the FHN model and the conventional integrate-and-fire model lies in the fact that the former has a nonlinear leakage coefficient.

From the data shown in Figs. 5 and 10 we might envisage that Kramer's formula, a special case of the large deviation theory (see Albeverio, Feng & Qian, 1995, and references therein for details) can predict the model behaviour. Kramer's model (Risken, 1989) reads

$$\langle T\rangle \sim \frac{2\pi}{\sqrt{H''(v_{\min})|H''(v_{\max})|}}\exp[2(H(v_{\max}) - H(v_{\min}))/\sigma^2] \tag{5.11}$$

where

$$H(v) = \gamma\left[\frac{1}{4}v^4 - (\alpha+1)\frac{1}{3}v^3 + \frac{1}{2}\alpha v^2\right] + \frac{1}{2\beta}v^2 - \mu v \tag{5.12}$$

and $v_{\max}$, $v_{\min}$ are the local maximum and left local minimum of the dynamical potential well H.[2] Hence, $v_{\max}$ is the exact threshold of the IF-FHN model. As we mentioned before for the IF-FHN model, its behaviour does not substantially change if we set the threshold as a value inside $[v_{\max}, 1]$.

Fig. 7 shows an application of Kramer's formula to the IF-FHN model with correlated inputs. When the input is uncorrelated, $c = 0$, Kramer's formula gives a rough estimate, with an obvious discrepancy between numerical results and the theoretical estimate. Nevertheless, when a small correlation is added ($c \geq 0.005$), i.e. the IF-FHN model receives a more random input, Kramer's formula gives an excellent estimate. As one might expect, the mean inter-spike interval and standard deviation exhibit a linear relationship.

5.2. Comparison with other models

As aforementioned, to find a simplified model that captures the essential of biophysical models has been persistently pursued in the literature. Some examples are: Abbott–Kepler's model (Abbott & Kepler, 1990), the spike response

[2] Remembering that for a given dynamical system, if it could be expressed as $d\xi_t = -\text{grad}H(\xi_t)dt + \sigma dB_t$, the function H is called the (dynamical) potential of ξ_t.

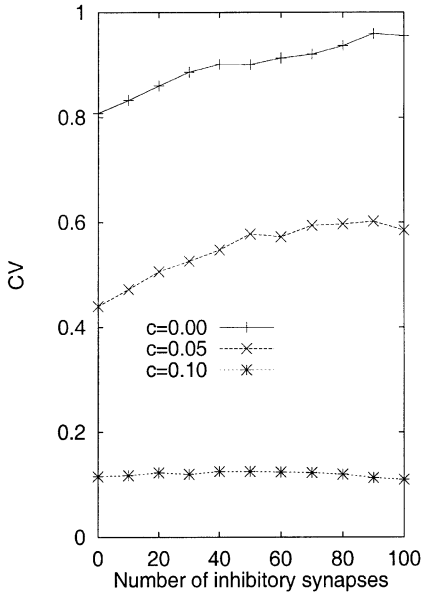

Fig. 6. CV versus q of the IF-FHN model. With fixed q, CV is a decreasing function of correlation c; in other words, the signal to noise ratio (SNR), SNR = 1/CV, is an increasing function of c, $p = 100$. Compare with Fig. 3.

model (Kistler et al., 1997) and, most recently, a model proposed in Stevens and Zador (1998b) with a decay depending on time. Among them, Abbott–Kepler's model is very close to the IF-FHN model and we carry out a comparison between them first.

The motivation to derive Abbott–Kepler's model is to fit the HH model with a nonlinear function which essentially results in an integrate-and-fire model with a nonlinear leakage. Abbott–Kepler's model is described by Eq. (5.5) in Abbott and Kepler (1990), i.e.

$$dV_t/dt = -0.250V_t + 0.083V_t^2 + 0.008V_t^3 + d\bar{i}_{syn}(t)/dt \tag{5.13}$$

with a threshold of 2.5. The IF-FHN model is

$$dv(t)/dt = -(1/\beta + \gamma\alpha)v(t) + \gamma(1+\alpha)v(t)^2 - \gamma v(t)^3 + d\bar{i}_{syn}(t)/dt \tag{5.14}$$

Let us now compare the leakage term of the IF-FHN model and Abbott–Kepler's model. In the IF-FHN model it is given by (see Eq. (5.9))

$$L_{\text{IF-FHN}}(v) = \gamma(v-1)(v-\alpha) + \frac{1}{\beta} \tag{5.15}$$

with a positive coefficient of v^2, but for Abbott–Kepler's model it is (see Figs. 4 and 8)

$$L_{\text{Abbott–Kepler}}(V_t) = 0.250 - 0.083V_t - 0.008V_t^2 \tag{5.16}$$

with a negative coefficient of V_t^2. Therefore, the overall dynamical properties of the two models are very different, with strong, positive current inputs there is only one attractor for the IF-FHN model which is finite (close to 1), while

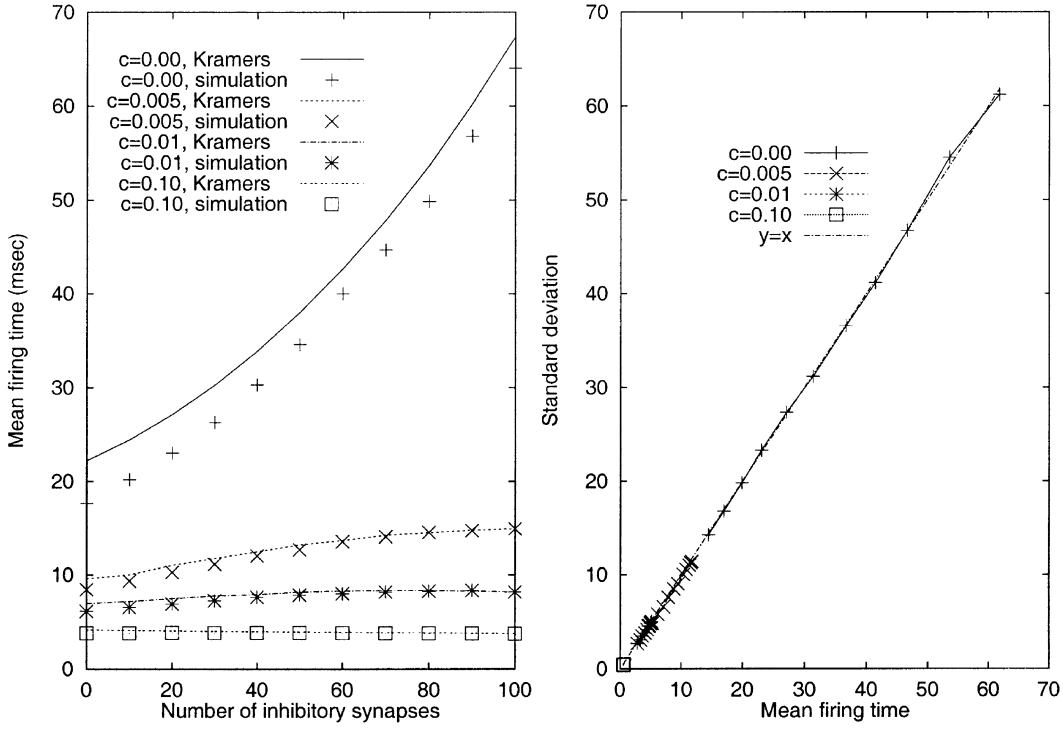

Fig. 7. A comparison between Kramer's formula and numerical simulations with parameters as specified in the context, $p = 100$.

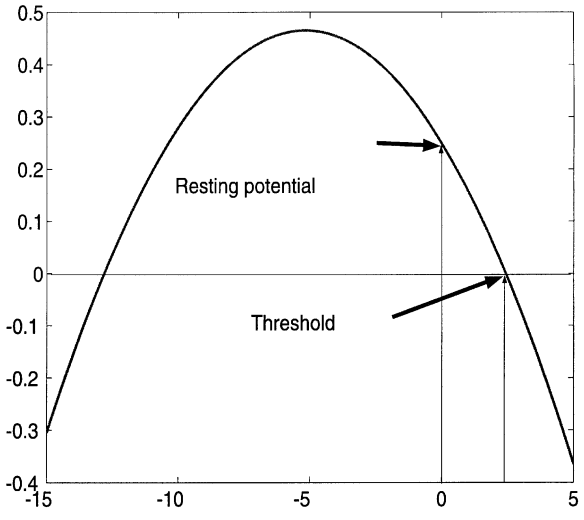

Fig. 8. $L_{\text{Abbott–Kepler}}(v)$ versus the membrane potentials. Between the threshold and the resting potential (indicated by arrows), $L_{\text{Abbott–Kepler}}(v)$ are positive, but the closer the membrane potential to the threshold, the weaker the leakage, in contrast to the conventional integrate-and-fire model. Compare with Fig. 4.

there are two attractors for Abbott–Kepler's model and both of them are infinite, i.e. $-\infty$ and ∞. The implication is that when simulating Abbott–Kepler's model with random inputs, we have to set a low boundary to prevent the membrane going to $-\infty$, but not for the IF-FHN model, similar to biophysical models such as the HH model. From a purely dynamical system point of view, the IF-FHN model could be a system with double potential wells (see footnote 2), but Abbott–Kepler's model has at most only one finite potential well.

As in the literature (Rinzel & Ermentrout, 1998), for a neuronal model defined by

$$\mathrm{d}v/\mathrm{d}t = f(v) + I$$

its v-nullcline is given by the function $f(v)$, where f is an appropriately defined function. Another difference between the two models is that the v-nullcline of the IF-FHN model takes the well known 'N' shape of biophysical neuron models (see for example, Fig. 7.3, p. 263 in Rinzel & Ermentrout, 1998), but in Abbott–Kepler's model it does not,[3] as shown in Fig. 9.

However, locally, the two models do share the same property: the closer the membrane potential to the threshold, the weaker the leakage, in contrast to the conventional integrate-and-fire model.

Finally, we mention here the possibility of further improvements of the approximation of the IF-FHN model to the FHN model. Remembering in Eq. (5.7) we only expand the term $\delta\int_0^t v(s)\exp(-\beta\delta(t-s))\mathrm{d}s$ to its first

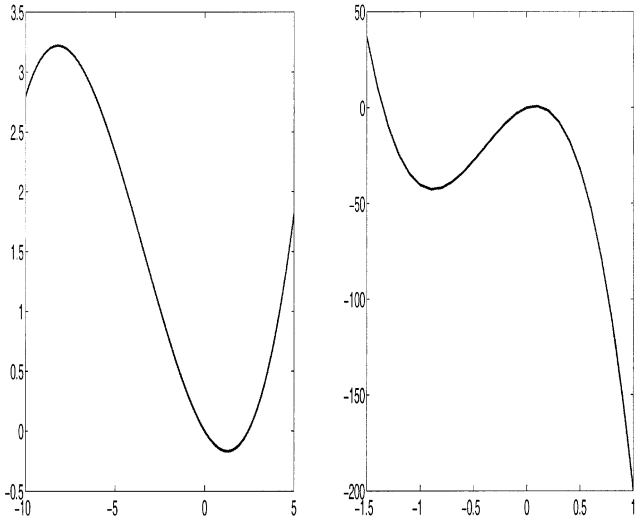

Fig. 9. v-nullcline in Abbott–Kepler's model (left) and the IF-FHN model (right). Note that they simply take opposite shapes.

order, using Taylor expansion, we could further obtain (see footnote 1)

$$\begin{aligned} v^{(1)}(t) = &-\left[\gamma(v-1)(v-\alpha) + \frac{\gamma}{\beta}(1-\exp(-\beta\delta t))\right]v(t) \\ &- \gamma\delta\sum_{n=1}^{\infty}\frac{v^{(n)}}{n!}\int_0^t (s-t)^n\exp(-\beta\delta(t-s))\mathrm{d}s \\ &+ \mathrm{d}\bar{i}_{\text{syn}}(t)/\mathrm{d}t \end{aligned} \tag{5.17}$$

As we have pointed out before, the IF-FHN model is only an approximation to the FHN model. In the FHN model, there are terms that depend on $v^{(i)}$ and are not leakage at all, i.e. it cannot be expressed in the form of $L(v)v$, where $L(v)$ is a bounded function.

Eq. (5.17) is a dynamical system of single variable and we could ask, for example, how many terms of $v^{(n)}$ are needed to reasonably approximate the FHN model. Furthermore, as in the spike response model (Kistler et al., 1997), we could also expand $v(s)$ according to some kernel functions rather than trivially using Taylor expansion, which could improve the efficiency of approximation.

Next, we turn our attention to the spike response model (Kistler et al., 1997). For the transparency of notation, we only take into account a simple version of the spike response model which is defined by

$$u(t) = \eta(t-t^f) + \int_0^{t-t^f}\epsilon(t-t^f,s)I(t-s)\mathrm{d}s \qquad t > t^f \tag{5.18}$$

where η, ϵ are defined[4] as in Kistler et al. (1997), t^f is the

[3] More appropriately, we should say that the v-nullcline takes reversal N-shape in the IF-FHN and other neuronal models, but takes N-shape in Abbott–Kepler's model. Nevertheless, in line with the terminology in the literature, we say that the v-nullcline in the IF-FHN model is N-shaped.

[4] Thanks to Dr Kistler for his courtesy to provide the exact form of functions η and ϵ.

most recently previous spiking time, and $\int_0^t I(s)\mathrm{d}s = \mu t + \sigma B_t$. More precisely, for ϵ we have

$$\begin{aligned}\epsilon(t-t^f,s) = [&0.10079\exp(-4.657s)\\ &+ 0.900395\cos(0.38307s)\exp(-0.2027s)\\ &- 0.0011869\exp(-0.1206599s)\\ &- 0.06177348\exp(-0.2027s)\sin(0.38307s)]\end{aligned}$$

$$\Theta(t-t^f) = \epsilon(s)\Theta(t-t^f) \tag{5.19}$$

where Θ is the Heaviside step function with $\Theta(s) = 1$ for $s > 0$ and 0 otherwise. From the property of Brownian motion, we know that $I(t-s) = \mu + \sigma \mathrm{d}B_{t-s}$ and so the model defined by Eq. (5.18) becomes

$$u(t) = \eta(t-t^{\mathrm{f}}) + \mu\int_0^{t-t^{\mathrm{f}}} \epsilon(s)\mathrm{d}s + \sigma\int_0^{t-t^{\mathrm{f}}} \epsilon(t-t^{\mathrm{f}}-s)\mathrm{d}B_s \tag{5.20}$$

Therefore, after the model emits a spike at time t^f, it is a nonhomogeneous Ornstein–Uhlenbeck process with a mean $\eta(t-t^f) + \int \epsilon(s)\mu\mathrm{d}s$ and variance $\int \epsilon^2(t-t^f-s)\sigma^2\mathrm{d}s$.

One obvious difference between the IF-FHN model and the spike response model is that after each spike the membrane potential of the former has to be manually reset to the resting potential, but not for the latter. After emitting a spike, the membrane potential in the spike response model returns to its resting potential due to the term $\eta(t)$. On the other hand, the process defined by the IF-FHN model is not a linear process, while the version of the spike response model defined here is a linear model per se—a nonhomogeneous Ornstein–Uhlenbeck process.

Finally, the motivation of deriving the IF-FHN model and Abbott–Kepler's and the spike response models is different. For the IF-FHN model, we aim to approximate the FHN model which itself is an approximation to the HH model. For both Abbott–Kepler's and the spike response models, the aim is to approximate the HH model, which is a more challenging task.

6. Examples: IBF

We use the following set of parameters in simulations (Brown et al., 1999) for the IF-FHN model:

$$\gamma = 100; \qquad \alpha = 0.2; \qquad \beta = 2.5$$

$v_{\mathrm{thre}} = 1$ and $v_{\mathrm{rest}} = 0$, as before.

For simplicity of notation we use $\lambda = p\lambda_{\mathrm{E}}$, $a = b$ and $T(r) = T$, where $r = q/p$. In Fig. 10 we see that when the excitatory input frequency is high ($\lambda = 5$ kHz), the output firing rate is a decreasing function of inhibitory input rate, in agreement with our intuitions. For example, when $r = 0$, $\langle T(0)\rangle + T_{\mathrm{ref}} = 6.33$ ms and $r = 1$, $\langle T(1)\rangle + T_{\mathrm{ref}} = 8.32$ ms. When the excitatory input frequency (λ) is around 3.8 kHz, the output firing rate is almost a constant function of inhibitory input rate. For example when $r = 0$, $\langle T(0)\rangle + T_{\mathrm{ref}} = 14.36$ ms and $r = 1$, $\langle T(1)\rangle + T_{\mathrm{ref}} = 14.26$ ms. Further reducing the excitatory input rate shows the IBF phenomenon: *increasing inhibitory inputs increases neuronal firing rates*. For example when $r = 0$, $\langle T(0)\rangle + T_{\mathrm{ref}} = 57.17$ ms and $r = 1$, $\langle T(1)\rangle + T_{\mathrm{ref}} = 29.87 + \mathcal{T}_{ref} = 29.87$ *ms*.

Let us define a *critical input frequency* λ_{c} as the quantity which satisfies

$$\langle T(0)\rangle = \langle T(1)\rangle \tag{6.1}$$

The numerical results of Fig. 10 tell us that λ_{c}~3.8 kHz when $a = 0.1$.

It has been widely reported in the literature that increasing inhibitory input to a neuron could increase the variability of its output (Brown et al., 1999; Shadlen & Newsome, 1994; Softky & Koch, 1993). Fig. 10 (right) shows standard deviation versus mean firing time $\langle T(r)\rangle$. As we reported before (Brown et al., 1999), the standard deviation of $T(r)$ almost equals its mean. Therefore, in the no IBF parameter regions, increasing inhibitory input induces an increase of its variability of output. However, in the parameter regions in which the IBF occurs, we see that now the coefficient of variation (CV) of $T(r)$ is a decreasing function of r rather than an increasing function of r, in contrast to conventional theory in the literature (see Fig. 11).

7. Theoretical results: IBF

Roughly speaking, the IBF phenomenon is due to a competition between two driving forces of neurons: stochastic and deterministic (Fig. 3). Assume that a is the magnitude of EPSPs (excitatory postsynaptic potentials) or IPSPs (inhibitory postsynaptic potentials) and λ is the input frequency. When the neuron receives purely excitatory inputs, the deterministic force is proportional to $a\lambda$ and the stochastic force is $a^2\lambda$. For the exactly balanced input case, the deterministic force is 0 and stochastic force is $2a^2\lambda$. In general, the deterministic force is more efficient in driving a cell to fire and, therefore, increasing inhibitory input reduces the firing rate of a neuron, in agreement with our intuition. However, when λ is small enough, the deterministic force of purely excitatory inputs is $a\lambda$ and the deterministic force plays a minor role in driving the cell to fire. In other words, now the noise term is more prominent. The noise term for the exactly balanced input case is $2a^2\lambda$, which is twice that for purely excitatory inputs, $a^2\lambda$. Therefore, under these circumstances the neuron fires faster when inhibitory inputs increase, i.e. noise increases. Nevertheless, we want to emphasize that the conclusions above are true only for diffusion type inputs. For the IF model with pulsatile EPSP and IPSP inputs, we see that it is impossible for any incoming IPSP to push the membrane up.

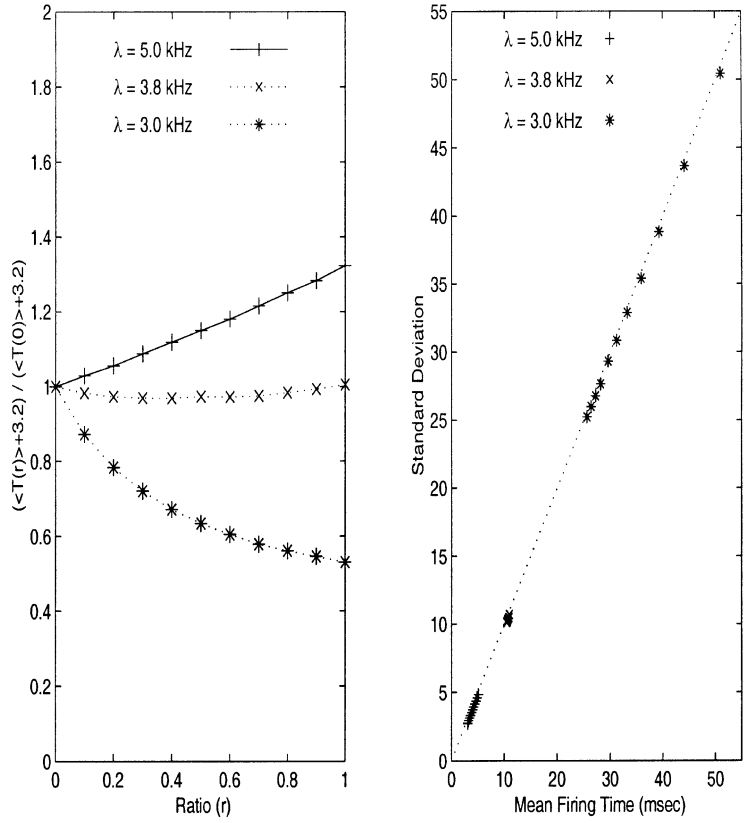

Fig. 10. $a = 0.1$. Left: when $\lambda = 5$ kHz, $\langle T(0)\rangle + T_{\text{ref}} = 6.33$ ms; $\lambda = 3.8$ kHz, $\langle T(0)\rangle + T_{\text{ref}} = 14.36$ ms; $\lambda = 3$ kHz, $\langle T(0)\rangle + T_{\text{ref}} = 57.17$ ms. Right: standard deviation of $T(r)$ versus $\langle T(r)\rangle$. It is easily seen that the standard deviation is almost equal to $\langle T(r)\rangle$, namely the efferent spike trains are a Poisson process.

The above scenario provides us with the answer to the 'why' question. It is of equal importance to answer the 'when' question, since, in parameter regions where the IBF phenomenon occurs, the neuron might fire too slowly and has no physiological reality. For the IF model and in parameter regions used in the literature, this is truly the case. It is difficult to observe it if only numerical simulations are employed. This might also tell us that why the IBF phenomenon has never been reported in the literature. Nevertheless, for the IF-FHN model, there are physiologically reasonable regions of (a, λ) in which increasing inhibitory inputs increases the neuronal firing rate, as we have observed for the HH model and the FHN model. We fully characterize the region for the IF-FHN model. As we pointed out before, the nonlinear leakage in the IF-FHN model ensures that it behaves very differently from the IF model.

The arguments above also indicate that increasing inhibitory inputs boosting the neuronal firing rate is a universal phenomenon. Whether we could observe it or not in a physiologically plausible parameter region depends on neuronal parameters, or, for real neurons, on the environment in which they operate. Since a neuron usually receives a massive excitatory and inhibitory input, we hope our finding could shed new light on the coding problem (Gerstner, Kreiter, Markram & Herz, 1997) and suggest another functional role of inhibitory inputs (van Vreeswijk, Abbott & Ermentrout, 1994), or noise terms in signal inputs.

The main purpose of this section is to characterize the parameter regions of (a, λ) in which increasing inhibitory input increases neuronal firing rates. It, thus, gives us a complete picture of the integrate-and-fire model and IF-FHN model behaviour, and provides us with the answers to the 'when' and 'why' questions.

7.1. The IF model

As in Feng and Brown (2000a), we could use the large deviation theory (Albeverio et al., 1995) to estimate the mean firing time of the model. The obtained results are quite clear-cut. However, it is an approximation result and the accuracy is quite poor (not shown). Recently, we have developed a rigorous theory (Feng & Li, 2000) on the calculation of the mean firing time of a one-dimensional neuron model. We therefore adopt the rigorous approach here.

To this end, we first introduce some general notation. Consider a diffusion process defined by

$$\mathrm{d}X_t = \mu(X_t)\mathrm{d}t + \sigma(X_t)\mathrm{d}B_t \tag{7.1}$$

Let us introduce the following quantities

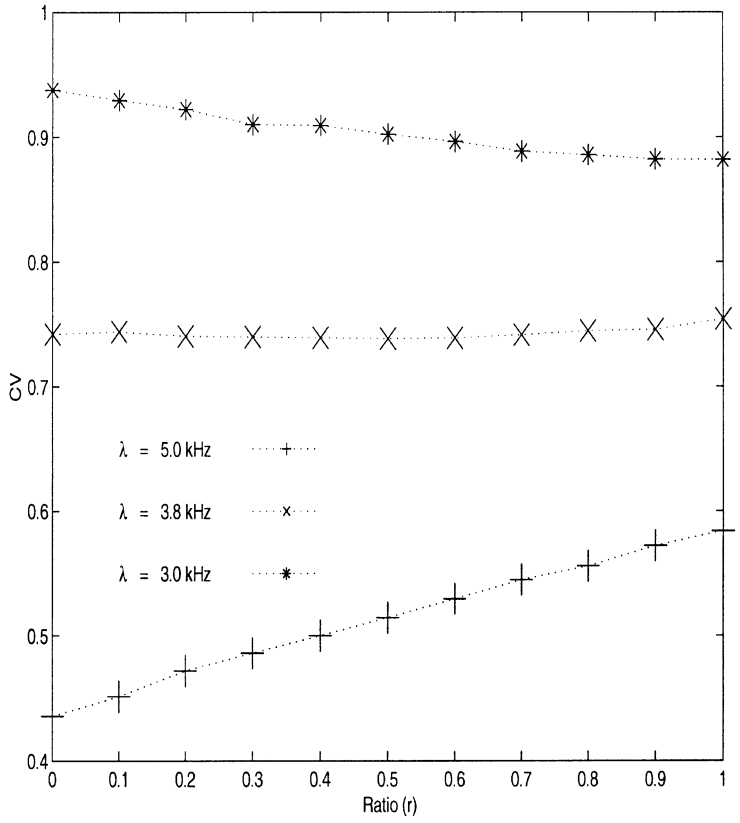

Fig. 11. Coefficient of variation (CV) of the IF-FHN model. CV can be either an increasing or a decreasing function of r.

$$s(x) = \exp\left(-\int_0^x \frac{2\mu(y)}{\sigma^2(y)}\mathrm{d}y\right),$$
$$m(x) = \frac{1}{s(x)\sigma^2(x)} = \frac{\exp\left(\int_0^x \frac{2\mu(z)}{\sigma^2(z)}\mathrm{d}z\right)}{\sigma^2(x)} \tag{7.2}$$

where m is the speed density, s the scale function. We call a diffusion process positive-recurrent if $\int_{-\infty}^{\infty} m(x)\mathrm{d}x < \infty$, which is equivalent to $\langle T\rangle < \infty$, where T is the first exit time of $(-\infty, V_{\text{thre}}]$. For a positive-recurrent process, its stationary distribution density is given by $\pi(x) \propto m(x)$.

The following conclusion is proved in Feng and Li (2000).

Theorem 1. For a positive-recurrent diffusion process X_t we have

$$\begin{aligned}\langle T\rangle &= 2\int_{V_{\text{rest}}}^{V_{\text{thre}}} s(u)\mathrm{d}u\cdot\int_{-\infty}^{V_{\text{rest}}} m(u)\mathrm{d}u + 2\\ &\quad\times\int_{V_{\text{rest}}}^{V_{\text{thre}}}\left(\int_y^{V_{\text{thre}}} s(u)\mathrm{d}u\right)\cdot m(y)\mathrm{d}y\\ &= 2\int_{V_{\text{rest}}}^{V_{\text{thre}}}\left(\int_{-\infty}^{y} m(u)\mathrm{d}u\right)\cdot s(y)\mathrm{d}y\end{aligned} \tag{7.3}$$

According to the definition of the scale function we have

$$s(x) = \exp\left(\frac{Lx^2 - 2a\lambda(1-r)x}{a^2\lambda(1+r)}\right) \tag{7.4}$$

and, therefore,

$$\langle T(r)\rangle = \frac{2}{L}\int_{\frac{V_{\text{rest}}\sqrt{L}}{a\sqrt{\lambda(1+r)}} - \frac{\sqrt{\lambda}(1-r)}{\sqrt{L}(1+r)}}^{\frac{V_{\text{thre}}\sqrt{L}}{a\sqrt{\lambda(1+r)}} - \frac{\sqrt{\lambda}(1-r)}{\sqrt{L}(1+r)}}\left[\exp(x^2)\int_{-\infty}^{x}\exp(-u^2)\mathrm{d}u\right]\mathrm{d}x \tag{7.5}$$

Eq. (7.5) has been derived earlier in Ricciardi and Sato (1990). The novelty of Theorem 1 lies in the fact that it is also applicable to other one-dimensional neuron models, as shown in the following sections for the IF-FHN model.

Hence, we have (see Feng & Li, 2000, for details)

Theorem 2. There is a unique critical input frequency $0 < \lambda_c < \infty$ satisfying

$$\langle T(0)\rangle = \langle T(1)\rangle \tag{7.6}$$

For the HH model, we know that inhibitory inputs can, in some circumstances, increase the firing rate, a phenomenon known as post-inhibitory rebound (PIR)[5] (Koch, 1999). With a Poisson input or its diffusion approximation, the

[5] However, to the best of our knowledge, PIR is reported only for neuronal models with deterministic inputs.

IBF is observable (see Section 10 on results with diffusion inputs). Nevertheless, we must emphasize here that the IBF for the IF model is a consequence of diffusion approximation. It is easily seen that with a Poisson input, the IBF for the IF model is not observable. The IF model with diffusion type inputs reconciles itself with the HH model in the sense that the IBF phenomenon is observable for both models. Unfortunately, for the IF model, a close check tells us that in parameter regions of input in which the IBF occurs, the efferent firing rate is far too low.

7.2. IF-FHN model

Applying Theorem 1 to the IF-FHN model, we obtain

$$s(x) = \exp\left[\int_0^x \frac{2L(y)y - 2\mu}{\sigma^2} \mathrm{d}y \right]$$
$$= \exp\left[\frac{\gamma}{2\sigma^2}x^4 - \frac{2(V_{\text{thre}} + \alpha)\gamma}{3\sigma^2}x^3 \right. \tag{7.7}$$
$$\left. - \frac{\alpha\gamma\beta V_{\text{thre}} + 1}{\sigma^2\beta}x^2 + \frac{2\mu x}{\sigma^2} \right]$$

and

$$m(x) = \frac{1}{\sigma^2}\exp\left[- \frac{\gamma}{2\sigma^2}x^4 + \frac{2(V_{\text{thre}} + \alpha)\gamma}{3\sigma^2}x^3 \right.$$
$$\left. - \frac{\alpha\gamma\beta V_{\text{thre}} + 1}{\sigma^2\beta}x^2 + \frac{2\mu x}{\sigma^2} \right] \tag{7.8}$$

However, a fully theoretical treatment of these quantities, as in the previous subsection, is difficult because of the nonlinearity of the leakage coefficient. Different from the integrate-and-fire model, now Kramer's formula gives a quite good approximation result, as shown before and in the next section. Due to the computational advantage of Kramer's formula, we concentrate on it in the following theoretical development for IF-FHN model.

We have used a geometrical method to prove the following conclusion (Feng & Li, 2000).

Theorem 3. For the IF-FHN model, there is a λ_c with the property that

$$\langle T(0)\rangle = \langle T(1)\rangle$$

8. Numerical results: IBF

For the integrate-and-fire model, Eq. (7.5) agrees perfectly with numerical results, as shown in Fig. 12(a). Parameters used in the simulations are $\lambda = 10$ kHz, $a = 0.5$ mV, $V_{\text{thre}} = 20$ mV, $V_{\text{rest}} = 0$, and $L = 1/20.2$.

Fig. 12(b) shows a comparison between numerical simulations and results obtained in terms of Kramer's formula

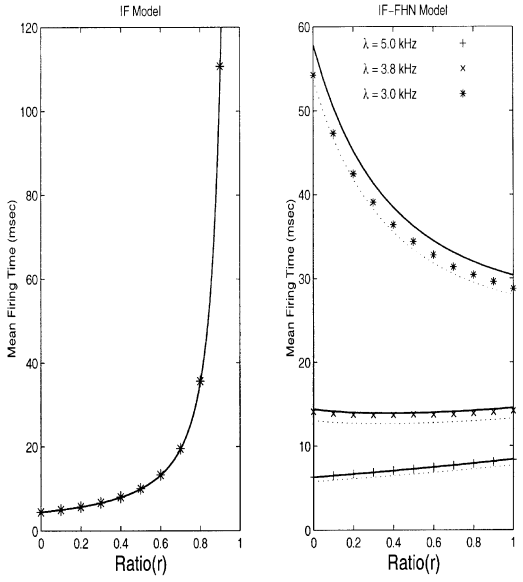

Fig. 12. (a) A comparison between Eq. (7.5) and numerical results of the integrate-and-fire model. Points are simulation results; the line represents the exact values by theory. (b) A comparison between Kramer's formula and numerical results of the IF-FHN model. Points are simulation results; dotted lines represent the approximations by Kramer's formula; solid lines represent the direct numerical evaluation of the integral in Theorem 1.

(see also figures in Section 5). We can see that there is a discrepancy between them, although in general they agree with each other. Moreover, numerical results are in agreement with the large deviation theory (Albeverio et al., 1995) which indicates that

$$\lim_{\lambda\to 0} \sigma^2 \log\langle T(r)\rangle = 2[H(v_{\max}) - H(v_{\min})]$$

Let us now, in terms of Kramer's formula, characterize the whole parameter regions of (a, λ) in which inhibitory inputs increase neuronal firing rates for the IF-FHN model.

Fig. 13 shows the curve of λ_c versus a for $0.02 \le a \le 0.1$. For example, when $a = 0.08$ we have $\lambda_c = 4.6$ kHz and a neuron fires at a rate of 38 Hz. When $\lambda \le \lambda_c$, increasing inhibitory input enhances the neuronal firing rates. In general, we see that when the input frequency is small, the inhibitory input increases the neuronal activity. Therefore, with the help of inhibitory inputs, a neuron's actively modulates its activity: when the input is high, inhibitory input decreases its firing; when input is low, inhibitory input increases its firing.

9. Correlated inputs: IBF

In previous sections, we considered the integrate-and-fire model and the IF-FHN model with independent inputs. Nevertheless, as we have pointed out before, a neuron usually receives spatially correlated inputs, rather than independent inputs (Stevens & Zador, 1998a). In this section, we consider the impact of correlated inputs on the IBF phenomenon.

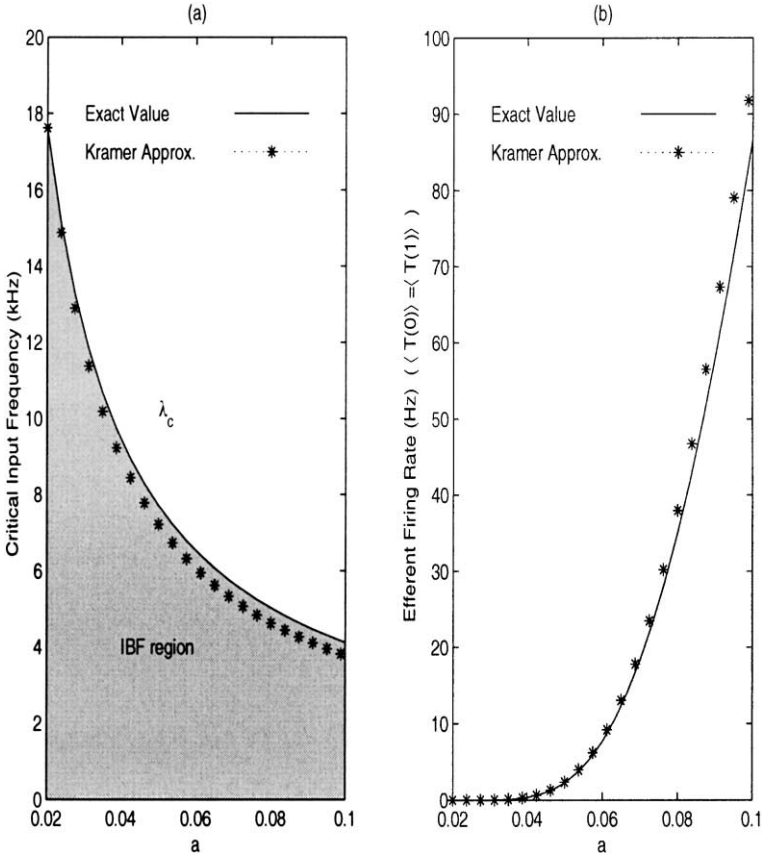

Fig. 13. (a) λ_c versus a for the IF-FHN model. (b) Efferent frequency when $\lambda = \lambda_c$ versus a.

The correlation between synapses increases the noise term, but keeps the mean input unchanged. As we pointed out before, the IBF phenomenon is due to a competition between the noise force and the deterministic force. We could naturally expect that increasing correlation, or the noise force, will facilitate the IBF phenomenon.

Fig. 14 presents numerical results further explaining the conclusions above. Even with a small correlation ($c = 0.05$), the IBF region for the IF-FHN model is considerably enlarged, compared with the case of $c = 0$. Assume that a neuron fires with its maximum rate of 500 Hz. We see from Fig. 14 that when $a \geq 0.03$ (approximately), $\lambda < \lambda_c$, namely all physiologically plausible parameters of inputs are inside the IBF region.

As we can see from Fig. 14 and previous numerical results, in the reasonable parameter ranges, the Kramer formula offers a fairly good approximation. Denote $\lambda_c^*(x)$, $x \in [0, 1]$ the correlation coefficient, as the Kramer approximation of the critical input frequency at which

$$\langle T(0)\rangle = \langle T(1)\rangle$$

we have

Theorem 4. For IF-FHN model, with the assumption of unique critical input frequency, if $c_1 > c_2$, then

$$\lambda_c^*(c_1) > \lambda_c^*(c_2)$$

Theorem 4 follows from the simple observation that $F(\mu)$ is independent of c and

$$\exp\left[\frac{2(H(v_{\max}) - H(v_{\min}))}{a^2\bar{\lambda}p(1 + c_1(p-1))(1+r)}\right] < \exp\left[\frac{2(H(v_{\max}) - H(v_{\min}))}{a^2\bar{\lambda}p(1 + c_2(p-1))(1+r)}\right]$$

when $c_1 > c_2$.

Similar conclusions hold true for the integrate-and-fire model as stated in the following theorem.

Theorem 5. For the integrate-and-fire model, if $c_1 > c_2$ then

$$\lambda_c(c_1) > \lambda_c(c_2)$$

10. Response surfaces

Neurons have traditionally been characterized by the

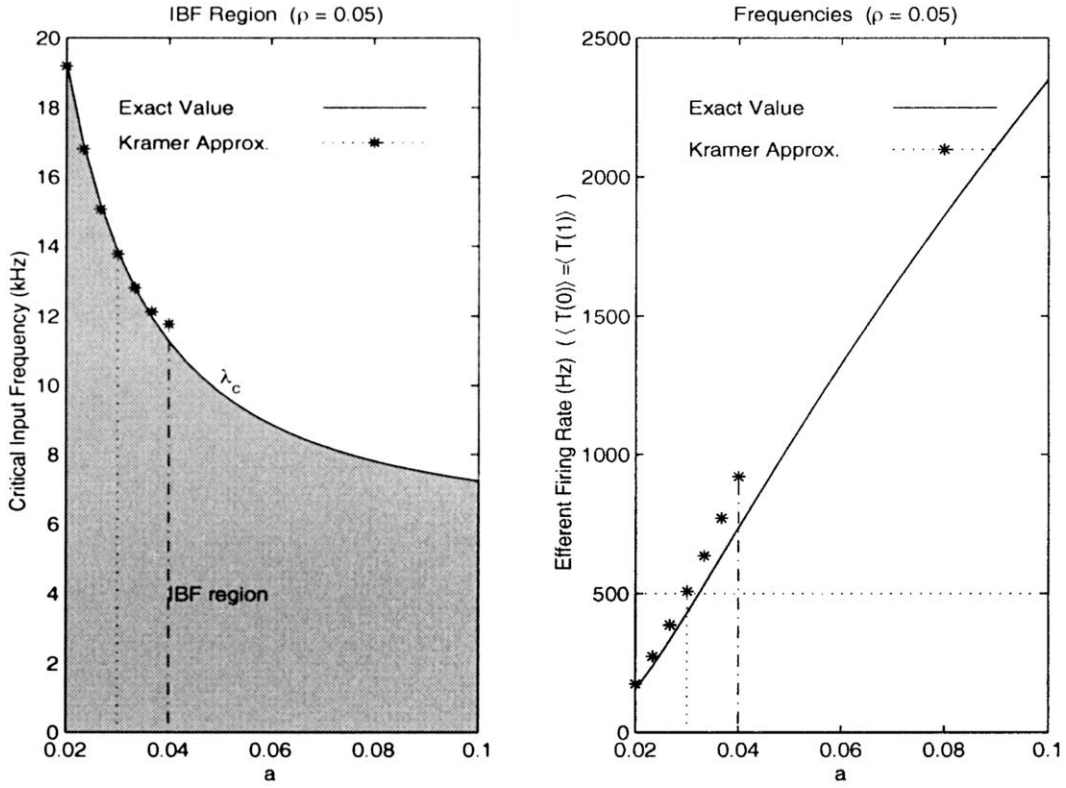

Fig. 14. λ_c versus a for the IF-FHN model and efferent frequencies $\langle T(0)\rangle = \langle T(1)\rangle$ when $\lambda = \lambda_c$ versus a, $\rho = c$. Note that to ensure the efferent frequencies are in physiologically plausible ranges, i.e. efferent firing rates ($\leq$500 Hz), when $a > 0.03$ ($\lambda_c < 13.856$), λ is in the IBF region.

nature of their so-called ω–I curve, that is the relationship between the rate of firing, ω, that they adopt in response to an applied current and the level of the applied current, I, proposed by Hodgkin. He classified membranes as type I, if they can show an arbitrarily low firing rate and long spike latency in response to a continuous current; or type II, if they exhibit a narrow range of response firing rates (not close to zero), and virtually zero spike latency. The HH model is classified as type II. In a sense, the IF model can be classified as type I, since arbitrarily low firing rates are possible for just supra-threshold currents. This is a useful categorization for many purposes, yet frequently neurons are subject to input regimes that cannot be approximated as a constant current, as we consider here. Inputs are often pulsatile, and, in numerous brain areas, e.g. the visual cortex and the hypothalamus, neurons fire apparently randomly. For a neuron model with stochastic inputs, the ω–I curve only provides us with limited information.

We thus propose a simple characterization of neuronal response to random synaptic input. This involves a graphical representation of the first two moments, the mean and variance, of neuronal output as a function of the first two moments of total synaptic inputs, for a range of values of these input moments. The usual approximations of a wide variety of stochastic input process are first constructed using the usual diffusion approximation (see Eq. (3.3)). The measures of mean and variability of output we use are conventional measures: overall firing rate ω and CV. Hence, when a neuron model receives inputs ranging from exactly balanced inputs to purely excitatory inputs, its behaviour can be fully understood by simply looking up the trajectory on the surface.

Applying the approach to the HH model and the IF model yields response surfaces as depicted in Fig. 15. Lines[6] (A–E) are trajectories for efferent firing frequency and CV, when μ goes from 0 (exactly balanced input) to $a\lambda_E p$ (purely excitatory input) or, equivalently, r from 0 to 1. We can easily tell the different response behaviour of the two models. Lines (A–E) cross contours of the CV–(μ, σ) surface of the IF model, but they are almost parallel with the contours of the HH model. Comparison of (A–E) in Fig. 15 demonstrates the huge changes in the noise component, σ, as a result of introducing very low correlation. The increase is greatest changing from $c = 0$ to $c = 0.01$, and, for the HH model, the consequent increase in ω is largest. At balance ($\mu = 0$), ω increases from 16 to 29 Hz, whereas for pure excitation input, the change is from 34 to 43 Hz, a rather smaller increase. Each subsequent equal sized increment in correlation induces lower increases in ω (e.g. to 37, 39, 41 Hz at balance) for two reasons: the increment in σ is

[6] All parameters are the same as in the previous sections, see Fig. 1.

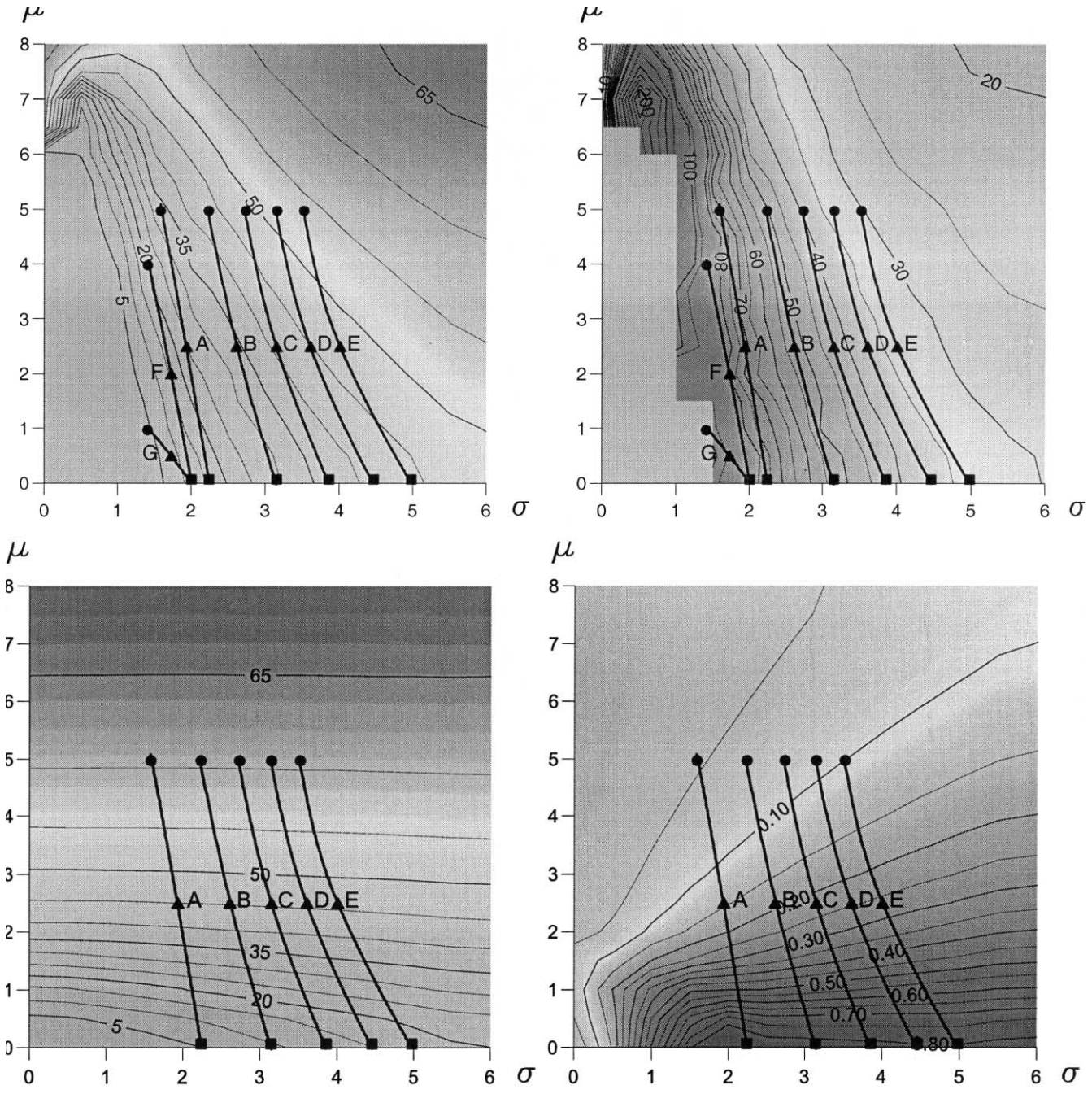

Fig. 15. Response surfaces of the HH and IF models with correlated inputs $c = 0$. (A), $c = 0.01$ (B), $c = 0.02$ (C), $c = 0.03$ (D), $c = 0.04$ (E) and $p = 100$, $a = b = 0.5$. In (F) $p = 80$ and $a = b = 0.5$, (G) $p = 5$ and $a = 2$. Top panel: left is ω–(μ, σ), right is CV–(μ, σ) for the HH model; middle panel: left is 2 ω–(μ, σ), right is CV–(μ, σ) for the IF model without a refractory period; bottom panel: left is ω–(μ, σ), right is CV–(μ, σ) for the IF model after adding a refractory period of 12 ms, which is approximately the refractory period of the HH model (Brown et al., 1999).

much lower at higher correlations (there are equal sized increments in σ^2), and the relationship between ω and σ has a lower slope at higher values of σ. However, for different values of p and a, and, therefore, different starting points on the μ, σ surface for independent inputs, the qualitative pattern of correlation-induced increments in ω might be very different. For the IF model, positive correlation increases ω, but by a much smaller amount (by virtually zero for purely excitatory input for the IF model). The effect on CV is the opposite to that for the HH model: it increases variability rather than reduces it, over much of the range.

As an application of the response surface approach, we show here that the IBF phenomenon for the HH model can be easily demonstrated by simply looking up the surface. Traces (F) and (G) in Fig. 15 depict two cases

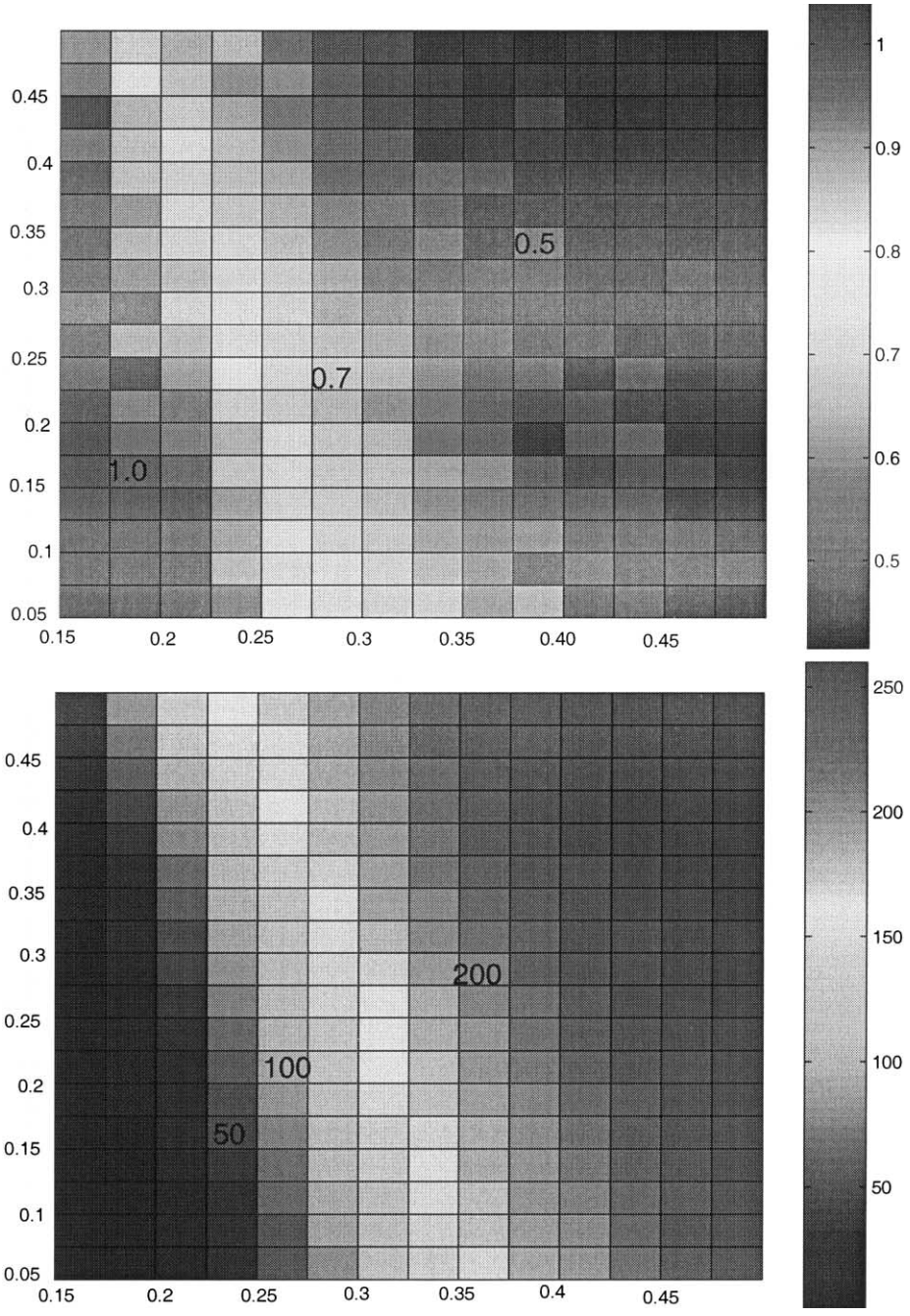

Fig. 16. Response surface of the IF-FHN model. Top panel is CV$-(\mu, \sigma)$ (the low left corner corresponds to high value) and bottom panel is $\omega-(\mu, \sigma)$ (the low left corner corresponds to low value). As in Fig. 15, the x-axis is σ and the y-axis is μ. As before, a refractory period of 3.2 ms is added for calculating mean and CV.

where the noise components at exact balance are equal, but as the inhibitory input is reduced the two cases diverge, the slope of (G), with larger EPSPs, being lower. The slope in (G) is so small that increasing inhibition (from $r = 1$ to $r = 0$) actually *increases* the firing rate from under 5 Hz to over 10 Hz. Increasing the inhibition induces a reduction in μ, but also a big increment in σ. These have opposite effects on the firing rate, ω. A net increase in ω occurs because the increase in ω due to the increase in σ is greater than the decrease due to the reduction in μ. Any change in the synaptic input that induces relative changes in μ and σ such that the slope of the trajectory is less steep than the contours of ω will result in a reduction of ω. This is most likely to occur in the region $5 < \omega < 20$, on the left of the figure for $1 < \sigma < 2$ and $0 < \mu < 6$, where contours of ω are

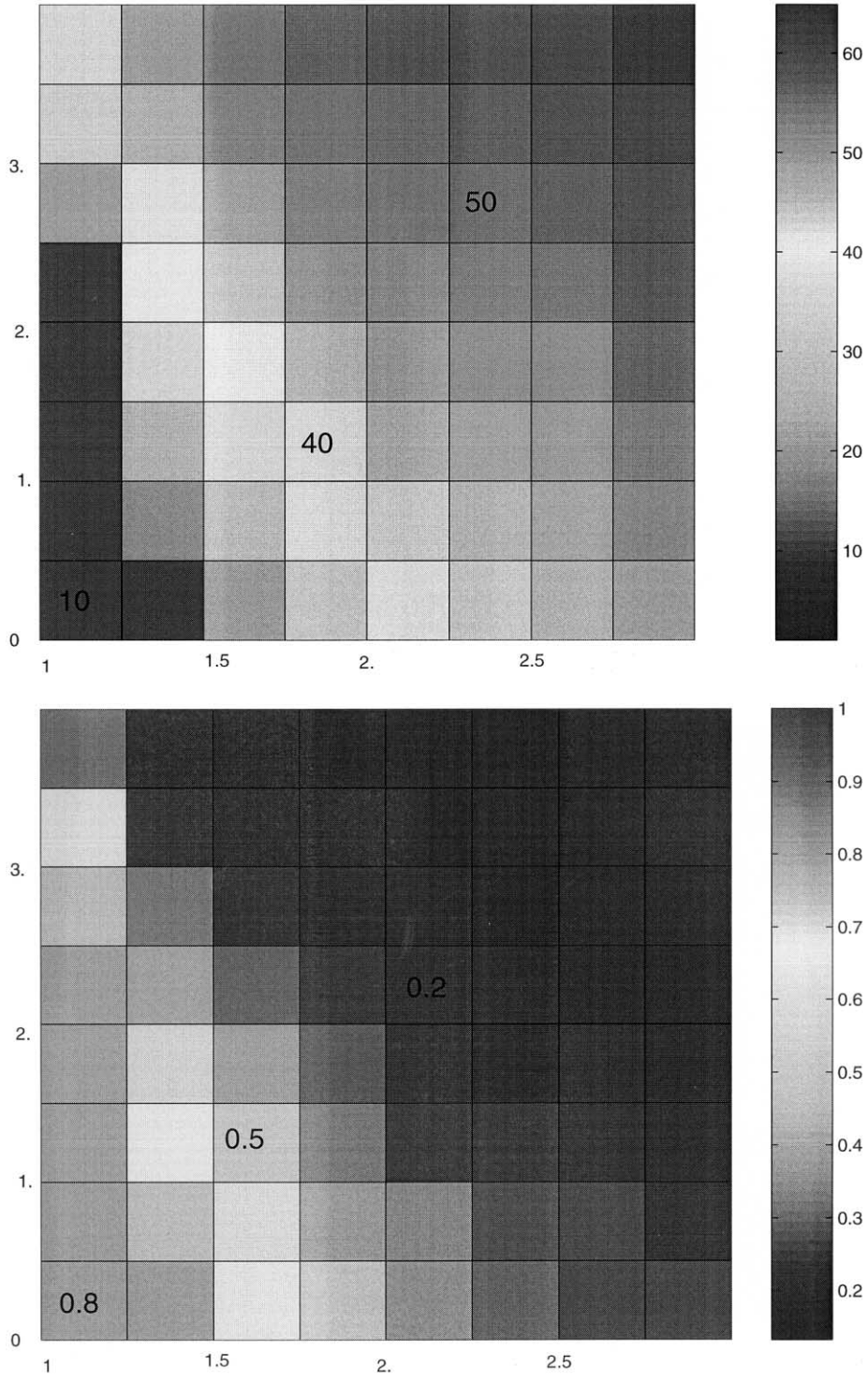

Fig. 17. Response surface of the spike response model. Top panel is CV$-(\mu, \sigma)$ (the low left corner corresponds to high value) and bottom panel is $\omega-(\mu, \sigma)$ (the low left corner corresponds to low value). As in Fig. 15, the x-axis is σ and the y-axis is μ. The model is numerically solved with a step of 0.2 ms and the threshold is 4.7 mV.

most steeply sloping. Shallow slopes in the trajectories corresponding to increase in inhibition are most likely to occur for large EPSP/IPSP sizes, and low EPSP/IPSP input rates. When the conjunction of these two features occurs, the IBF is most likely to occur. It is clearly indicated that with the increasing of inhibitory inputs, the output firing rate is almost doubled, from 5 to 10 Hz.

To further demonstrate the similarity between the IF-FHN model and the HH model, in Fig. 16 we plot the response surface for the IF-FHN model. It is easily seen

that Fig. 16 is similar to that of the HH model: the contours of both CV and mean of ISI follow the gradient of μ, while for the IF model they mostly follow the gradient of σ (see Fig. 15). Therefore, we could easily expect that the IBF model could also be observed in the IF-FHN model, as we demonstrated before. Nevertheless, note that the IF-FHN model is of Type I since it is a one-dimension and first order dynamical system. For type II model, which undergoes a Hopf bifurcation, we require a system of two or higher dimensions so that the eigenvalues could not be real (see Rinzel & Ermentrout, 1998, p. 259).

Finally, in Fig. 17 we plot the response surface for the spike response model defined in Section 5.2. It is interesting to see that the contours of mean firing rates and CV mostly follow the gradient of μ, as in the HH model and the IF-FHN model. Note that here we only consider the simplest version of the spike response model which approximates the HH model and we have not fully optimized all parameters in the model (threshold is 4.7 mV, but we have not considered another parameter, i.e. the time from threshold crossing to maximum of the action potential), as described in Kistler et al. (1997). Nevertheless, we can conclude that the phenomena reported in the previous sections are also true for the model. With the improvement of the approximation (outside of the present review paper, see Kistler et al., 1997), we expect that the response surface of the spike response model would more resemble that of the HH model.

11. Discussion

In summary, in Brown et al. (1999), independent inputs to neuronal models are considered and we assert that the IF model and the HH model behave *differently*. The present work carries this a considerable stage further in that, when correlated inputs are considered, the IF and HH models behave in totally *opposite* ways: the SNR of the IF model decreases with the increase of the input correlation; while the SNR of the HH model increases. The conclusions of the present work would be informative, in particular when we deal with network models where inputs to each unit are bound to be correlated. For a given neuron with stochastic inputs, the response surface provides us with a valuable way to understand its behaviour. Finally, using the IF-FHN model, we pointed out that the key difference between the IF model and the HH model is that the leakage coefficient is a constant for the former, but it depends on inputs for the latter. The difference between the IF model and the IF-FHN model might also provide a clue for the phenomenon observed in Azouz and Gray (2000).

The classical approach to neural networks is that excitatory neurons are the main information carriers. It is thought that neurons receive virtually all significant input from excitatory inputs, and that inhibitory neurons interact only locally and responsively. The stronger the (excitatory) inputs, the higher the output rate. When modelling, the conventional view is that information is received solely through excitatory inputs (EPSPs) (Abbott, Varela, Sen & Nelson, 1997), and that neurons process this information either by integration or coincidence detection (Softky & Koch, 1993). Inhibitory inputs are often thought of as broad dampening influences, usually reducing neuronal responsiveness to all input. The role of inhibitory inputs have been extensively discussed in recent years, and various functions have been postulated. These include the production of a more graded response to changes in input, and facilitating neuronal synchronization (van Vreeswijk et al., 1994). Substantial inhibitory input has also been demonstrated to be one factor that can induce increased random variability of neuronal output (Shadlen & Newsome, 1994). Here, we find a more surprising effect of inhibitory input: actually increasing the neuronal firing rate.

Finally we want to emphasize that now the time is ripe to replace the classic IF model with a constant leakage coefficient by the IF-FHN model with a nonconstant leakage coefficient. The IF-FHN model is easy to simulate and embodies some essential properties of biophysical models. In the literature, there are a few simplified versions of biophysical neuron models including Abbott–Kepler's model and the spike response model. Locally, closing the threshold, the IF-FHN shares similar dynamical properties with Abbott–Kepler's model, but the global dynamics between them is very different. In terms of the first and second statistics of inter-spike intervals, the spike response model well mimics the HH model, but it requires more computational resources than the IF-FHN model.

Acknowledgements

I thank David Brown, Stuart Feerick and Guibin Li for their collaborations on different topics reviewed here, and Wulfram Gerstner for his many valuable comments on early versions of this manuscript. The work was partially supported by BB-SRC, a grant of the Royal Society and an EU grant.

References

Abbott, L. F. (1994). Single neuron dynamics: an introduction. In F. Ventriglia, *Neural modelling and neural networks* (pp. 57–78). Oxford: Pergamon Press.

Abbott, L. F., & Kepler, T. B. (1990). Model neurons: from Hodgkin–Huxley to Hopfield. In L. Garrido, *Statistical mechanics of neural networks* (pp. 5–18). Berlin: Springer-Verlag.

Abbott, L. F., Varela, J. A., Sen, K., & Nelson, S. B. (1997). Synaptic depression and cortical gain control. *Science*, *275*, 220–223.

Albeverio, S., Feng, J., & Qian, M. (1995). Role of noises in neural networks. *Physical Review E*, *52*, 6593–6606.

Albright, T. D., Jessell, T. M., Kandel, E. R., & Posner, M. I. (2000). Neural science: a century of progress and the mysteries that remain. *Cell*, *100*, s1–s55.

Azouz, R., & Gray, C. M. (2000). Dynamic spike threshold reveals a mechanism for synaptic coincidence detection in cortical neurons in vivo. *Proceedings of National Academy of Science USA*, *97*, 8110–8115.

Barlow, H. (1986). Perception: what quantitative laws govern the acquisition of knowledge from the senses? In C. Coen, *Functions of the brain* (pp. 11–43). Oxford: Clarendon Press.

Brown, D., Feng, J., & Feerick, S. (1999). Variability of firing of Hodgkin–Huxley and FitzHugh–Nagumo neurons with stochastic synaptic input. *Physical Review Letters*, *82*, 4731–4734.

Collins, J. J., Chow, C. C., & Imhoff, T. T. (1995). Stochastic resonance without tuning. *Nature*, *376*, 236–238.

Feng, J. (1997). Behaviours of spike output jitter in the integrate-and-fire model. *Physical Review Letters*, *79*, 4505–4508.

Feng, J., & Brown, D. (2000a). Integrate-and-fire models with nonlinear leakage. *Bulletin of Mathematical Biology*, *62*, 467–481.

Feng, J., & Brown, D. (2000b). Impact of correlated inputs on the output of the integrate-and-fire models. *Neural Computation*, *12*, 711–732.

Feng, J., & Li, G. (2000). Impact of geometrical structures on the output of neuronal models—a theoretical and numerical analysis. *Neural Computation* (accepted).

Feng, J., & Tirozzi, B. (2000). Stochastic resonance tuned by correlation in neuronal models. *Physical Review E*, *61*, 4207–4211.

Feng, J., & Zhang, P. (2001). The behaviour of the integrate-and-fire and the Hodgkin–Huxley models with correlated inputs. *Physical Review E*, *63*, 051902-1–051902-11.

Gammaitoni, L., Hänggi, P., Jung, P., & Marchesoni, F. (1998). Stochastic resonance. *Reviews of Modern Physics*, *70*, 224–287.

Gerstner, W., Kreiter, A. K., Markram, H., & Herz, A. V. M. (1997). Neural codes: firing rates and beyond. *Proceedings of Nation Academy of Science USA*, *94*, 12740–12741.

Hines, M. L., & Carnevale, N. T. (1997). The NEURON simulation environment. *Neural Computation*, *9*, 1179–1209.

Kistler, W. M., Gerstner, W., & van Hemmen, J. L. (1997). Reduction of the Hodgkin–Huxley equations to a single-variable threshold model. *Neural Computation*, *9*, 1015–1045.

Koch, C. (1999). *Biophysics of computation*. New York: Oxford University Press.

Konig, P., Engel, A. K., & Singer, W. (1996). Integrator or coincidence detector? The role of the cortical neuron revisited. *Trends in Neurosciences*, *19*, 130–137.

Matthews, P. B. C. (1996). Relationship of firing intervals of human motor units to the trajectory of post-spike after-hyperpolarization and synaptic noise. *Journal of Physiology*, *492*, 597–628.

Musila, M., & Lánskú, P. (1994). On the interspike intervals calculated from diffusion approximations for Stein's neuronal model with reversal potentials. *Journal Theoretical Biology*, *171*, 225–232.

Ricciardi, L. M., & Sato, S. (1990). Diffusion process and first-passage-times problems. In L. M. Ricciardi, *Lectures in applied mathematics and informatics* (pp. 206–285). Manchester: Manchester University Press.

Rinzel, J., & Ermentrout, B. (1998). Analysis of neural excitability and oscillations. In C. Koch & I. Segev, *Methods in neural modeling* (pp. 251–292). Cambridge, MA: MIT Press.

Risken, S. (1989). *The Foller–Planck equation*, Berlin: Springer-Verlag.

Salinas, E., & Sejnowski, T. (2000). Impact of correlated synaptic input on output firing rate and variability in simple neuron models. *Journal of Neuroscience*, *20*, 6196–6209.

Shadlen, M. N., & Movshon, J. A. (1999). Synchrony unbound: a critical evaluation of the temporal binding hypothesis. *Neuron*, *24*, 67–77.

Shadlen, M. N., & Newsome, W. T. (1994). Noise, neural codes and cortical organization. *Current Opinion in Neurobiology*, *4*, 569–579.

Shadlen, M. N., & Newsome, W. T. (1998). The variable discharge of cortical neurons: implications for connectivity, computation, and information coding. *Journal of Neuroscience*, *18*, 3870–3896.

Sheth, B. R., Sharma, J., Rao, S. C., & Sur, M. (1996). Orientation maps of subjective contours in visual cortex. *Science*, *274*, 2110–2115.

Softky, W., & Koch, C. (1993). The highly irregular firing of cortical cells is inconsistent with temporal integration of random EPSPs. *Journal of Neuroscience*, *13*, 334–350.

Stevens, C. F., & Zador, A. M. (1998a). Input synchrony and the irregular firing of cortical neurons. *Nature Neuroscience*, *1*, 210–217.

Stevens, C. F., & Zador, A. M. (1998). Novel integrate-and-fire model of repetitive firing in cortical neurons. In *Proceedings of the Fifth Joint Symposium on Neural Computation UCSD*. La Jolla, CA.

Tuckwell, H. C. (1998). *Introduction to theoretical neurobiology*, Cambridge, UK: Cambridge University Press.

van Vreeswijk, C., Abbott, L. F., & Ermentrout, G. B. (1994). When inhibition not excitation synchronizes neural firing. *Journal of Computational Neuroscience*, *1*, 313–321.

Zohary, E., Shadlen, M. N., & Newsome, W. T. (1994). Correlated neuronal discharge rate and its implications for psychophysical performance. *Nature*, *370*, 140–143.